AMERICAN SOCIETY FOR MICROBIOLOGY | Infection and Immunity

Host-Microbial Interactions | Full-Length Text

IFN-λ3 is induced by *Leishmania donovani* and can inhibit parasite growth in cell line models but not in the mouse model, while it shows a significant association with leishmaniasis in humans

Manjarika De,[1] Soumi Sukla,[2,3] Seema Bharatiya,[1,4] Sagar Keshri,[1,4] Debarati Guha Roy,[1,4] Sutopa Roy,[5] Debrupa Dutta,[2] Shriya Saha,[1] Sarfaraz Ahmad Ejazi,[6,7] V. Ravichandiran,[2] Nahid Ali,[6] Mitali Chatterjee,[5] Sreedhar Chinnaswamy[1,4]

AUTHOR AFFILIATIONS See affiliation list on p. 20.

ABSTRACT The intracellular protozoan parasite *Leishmania donovani* causes debilitating human diseases that involve visceral and dermal manifestations. Type 3 interferons (IFNs), also referred to as lambda IFNs (IFNL, IFN-L, or IFN-λ), are known to play protective roles against intracellular pathogens at the epithelial surfaces. Herein, we show that *L. donovani* induces IFN-λ3 in human as well as mouse cell line-derived macrophages. Interestingly, IFN-λ3 treatment significantly decreased parasite load in infected cells, mainly by increasing reactive oxygen species production. Microscopic examination showed that IFN-λ3 inhibited uptake but not replication, while the phagocytic ability of the cells was not affected. This was confirmed by experiments that showed that IFN-λ3 could decrease parasite load only when added to the medium at earlier time points, either during or soon after parasite uptake, but had no effect on parasite load when added at 24 h post-infection, suggesting that an early event during parasite uptake was targeted. Furthermore, the parasites could overcome the inhibitory effect of IFN-λ3, which was added at earlier time points, within 2-3 days post-infection. BALB/c mice treated with IFN-λ3 before infection led to a significant increase in expression of IL-4 and ARG1 post-infection in the spleen and liver, respectively, and to different pathological changes, especially in the liver, but not to changes in parasite load. Treatment with IFN-λ3 during infection did not decrease the parasite load in the spleen either. However, IFN-λ3 was significantly increased in the sera of visceral leishmaniasis patients, and the IFNL genetic variant rs12979860 was significantly associated with susceptibility to leishmaniasis.

KEYWORDS type III IFN, IFN-L3, *Leishmania donovani*, *Leishmania*, visceral leishmaniasis, post-kala-azar dermal leishmaniasis

Leishmaniasis is an important vector-borne disease of the tropics caused by the protozoan parasite *Leishmania* genus (1). Several species and sub-species of *Leishmania* cause debilitating diseases like visceral leishmaniasis (VL), cutaneous leishmaniasis, and post-kala-azar dermal leishmaniasis (PKDL) in humans. The disease is endemic in India (2). The parasite is transmitted to humans by the phlebotomine sand fly and has well-defined polymorphic forms in different stages of the life cycle. The sand fly injects the promastigote form of the parasite under the skin of a human, following which phagocytic cells take up the parasite actively, where the parasite undergoes metamorphosis and becomes the amastigote form. Even though neutrophils also phagocytose the parasites, it is macrophages where the parasite spends most of its time replicating

Editor Jeroen P. J. Saeij, University of California, Davis, Davis, California, USA

Address correspondence to Sreedhar Chinnaswamy, sc2@nibmg.ac.in.

Manjarika De and Soumi Sukla contributed equally to this article. The author order was decided alphabetically.

The authors declare no conflict of interest.

See the funding table on p. 20.

Received 4 December 2023
Accepted 11 December 2023
Published 9 January 2024

Copyright © 2024 American Society for Microbiology. All Rights Reserved.

while inside the host (3); where likely, it may use neutrophils as a "Trojan horse" to enter macrophages (4).

Laboratory mice have served as useful models to study *Leishmania* infections (5). BALB/c mice infected with *Leishmania donovani* are used as a model to study VL, even though it is a sub-clinical infection model, as the mice do not succumb to the infection (unlike untreated humans) but carry the parasite for life (6, 7). The infected mice show granuloma formation (8) and subsequently clear the parasite from the liver by 4 weeks after infection, while the parasite may persist for a long time within the spleen (6). While a number of factors determine the outcome of the infection, such as parasite genotype and dose and route of inoculation, the mice's genetic background is also a major contributor (6). Polymorphisms in the solute carrier family 11a member 1 (*Slc11a1*) and the major histocompatibility complex 2 (*H2*) genes make different laboratory strains of mice either susceptible or resistant to *Leishmania* infections (9). While BALB/c mice support an asymptomatic infection, the C57BL/6 are resistant to *Leishmania* infections owing to the induction of an M1 phenotype and related pathways in the infected macrophages (7). Genetic polymorphisms in the human hosts involving *MHC* classes 1–3, *SLC11A1, IL-4, TGFB, IFNGR1*, and others have also been reported to be associated with leishmaniasis in humans (9), while a genome-wide association study (GWAS) has identified *HLA-DRB1–HLA-DQA1* as the top hit in VL (10).

Type 3 interferons (IFNs), also known as lambda IFNs (IFNL, IFN-L, or IFN-λ), are the newest family of IFNs; three out of the four IFNL genes (*IFNL1-3*) present on chromosome 19 were identified after the completion of the human genome project in 2003 (11, 12), while the fourth (*IFNL4*) was identified in 2013 during follow-up studies to hepatitis C virus (HCV) GWAS (13). Although they were initially referred to as both interleukins (IL-28A, B, and IL-29 for IFNL-2, 3, and 1, respectively) (12) and IFNs (11), it has come to be common practice to refer to them as IFNs, owing to their antiviral properties and functions that are similar to the other two types (1 and 2) of IFNs (14). The striking difference between type 1 and type 3 IFNs—the two IFN types that can be produced by non-immune cells—is that the receptors for type 3 IFNs are exclusively distributed on epithelial cells and cells of epithelial origin, unlike type 1 IFNs, which act more ubiquitously (15). Type 3 IFNs are also produced by immune cells like plasmacytoid dendritic cells (DCs), while macrophages and DCs, but not monocytes, respond to them (16).

While type 3 IFNs have been extensively studied in viral infections, their roles in other pathogen infections, especially in bacterial and fungal diseases, are being revealed (17, 18). They have been implicated so far in at least two protozoan parasitic diseases: malaria and cryptosporidiosis, both in mouse models (19), while a genetic association with IFN-λ4 has been shown for malaria in African children (20). A recent preprint article has shown a protective role for IFN-λ3 in oral *Toxoplasma gondii* infection in mice (21). However, no studies, to the best of our knowledge, have been reported on the role of type 3 IFNs in *Leishmania* infections. Since the route of entry of the *Leishmania* parasite is skin/epidermis that has stratified squamous epithelial cells, since leishmaniasis manifests in dermal/cutaneous forms, and since the parasite dwells in macrophages, type 3 IFNs, which are the guardians of the epithelium (15), should have important roles to play in leishmaniasis development and progression. Moreover, our recent transcriptomics analysis has consistently shown "Leishmaniasis" as a significantly associated disease pathway that is activated in both M1 and M2 macrophages differentiated from human monocytes in the presence of either IFN-λ3 or IFN-λ4 or both (16, 22). In the present study, for the first time, we attempt to address the host-parasite interactions involving type 3 IFNs and *L. donovani* infections by using cell lines and mouse models, as well as in human patients.

MATERIALS AND METHODS

Cells and reagents

Human and mouse monocytic cell lines THP-1 and U937 (purchased in 2018 from ATCC, Manassas, VA, USA) were maintained in RPMI-1640 medium supplemented with 10% fetal bovine serum (FBS) and penicillin/streptomycin (all from Gibco, Waltham, MA, USA) at 37°C and 5% CO_2. RAW264.7 cells, a gift from Dr. Suvendra Nath Bhattacharyya (Indian Institute of Chemical Biology) through Dr. Anindita Ukil (Calcutta University) (originally from the National Center for Cell Sciences, Pune, India), were maintained in Dulbecco's Modified Eagle Medium (Gibco), with other conditions being the same as above. Human and mouse recombinant IFN-λ3, human IFN-λ4, human and mouse IL28B/IFN-L3, IL1-β, IL-10, TNF-α, IL-4, and IFN-γ DuoSet ELISA kits were from R&D Systems (Minneapolis, MN, USA). All other chemicals and reagents, including 2′,7′-dichlorofluorescein diacetate (DCFDA) and N-Acetyl-L-cysteine (NAC), were purchased from Sigma-Aldrich (St. Louis, MO, USA). QIAamp DNA Mini Kit and RNeasy Kit were from Qiagen, Hilden, Germany; TRIzol reagent; Verso cDNA Synthesis Kit and prolongTM gold antifade mountant with 4′,6-diamidino-2-phenylindole (DAPI) were purchased from Thermo Scientific, Waltham, MA, USA; CFSE-Cell Labeling Kit (ab113853), Phalloidin-iFluor 647 Reagent (ab176759), and Phagocytosis Assay Kit (Green Zymosan) (ab234053) were purchased from Abcam, Waltham, MA, USA; iTaq universal SYBR green supermix was from Bio-Rad, Hercules, CA, USA; SYBR green qPCR master mix, TaqMan mastermix and TaqMan gene expression assays were purchased from Applied Biosystems, Waltham, MA, USA; DNA oligos/primers were from IDT (Coralville, IA, USA). In blocking antibody, the rat anti-mouse IL28B/IFN-L3 was from R&D Systems. RNAqueous-4PCR Kit was from Ambion, Austin, TX, USA. Genotyping reagents were from LGC genomics, UK. The oligonucleotides used in the study are listed in Table S1.

Cell culture, parasite culture, and infection

THP-1/U937 cells were first differentiated into macrophage-like cells using 100 nM phorbol 12-myristate 13-acetate (PMA) for 48 h (16) before giving infections. RAW264.7 cells were directly infected. Promastigotes of *Leishmania donovani* strain AG83 [MHOM/IN/83/AG83 (ATCC PRA-413)] were cultured at 22°C in M199 (pH 7.4) (Sigma-Aldrich) with 10% heat-inactivated FBS and 1% penicillin/streptomycin and sub-cultured in the same medium at an average density of 2×10^6 cells/mL. Stationary-phase parasites were used for infections. The multiplicity of infection (MOI) was 1:10 unless specified. Recombinant IFN-λ3 was added at the concentrations indicated in the figures or legends at the stated time points, either during infection or after removing the uninfected parasites from the medium as specified in the relevant figures, legends, or text. The infection was allowed for 24, 48, or 72 h, as stated in the respective figures and legends; if not, the infection was for 24 h. After the specified infection period, cells were washed with phosphate buffered saline (PBS) three times to remove free parasites and harvested for various experiments; cell-supernatants were collected for enzyme-linked immunosorbent assay (ELISA).

Quantitative PCR and quantification of the parasite load in infected cells

For quantifying parasite load, DNA was isolated from infected cells, and parasite kinetoplast DNA (kDNA) and human *GAPDH* or mouse *Gapdh* regions were amplified in real time using SYBR green qPCR master mix (Applied Biosystems) in a Step One Plus Real-Time PCR system (Applied Biosystems). *GAPDH/Gapdh* was used as a housekeeping gene, and fold expression changes were calculated using the $2^{-\Delta\Delta Ct}$ method.

To measure host gene expression, total RNA was isolated using either the RNeasy kit or TRIzol reagent. RNA (500 ng) was converted to cDNA using the Verso cDNA Synthesis Kit. Gene-specific primers (Table S1), iTaq universal SYBR green supermix, and SYBR green qPCR master mix were used for quantitative PCR (qPCR). *IFNL3/Ifnl3* was also amplified from cDNA using TaqMan probes with the TaqMan master mix. TaqMan gene expression

assays for human *IFNL3* (assay ID: Hs04193049_gH), actin beta, and *ACBT* (assay ID: Hs01060665_g1); mouse *Ifnl3* (assay ID: Mm04204156_gH); and mouse ribosomal protein S29 (*Rps29*) (assay ID: Mm02342448_gH) were used. qPCR was performed using either the CFX96 Real-Time System (Bio-Rad) or the QuantStudio5 Real-Time System (Applied Biosystems). *GAPDH/Gapdh* (human and mouse)/*ACTB* (human) and mouse *Rps29* were used as internal controls, and relative expression was calculated using the $2^{-\Delta\Delta CT}$ method.

Microscopy

For confocal microscopy, THP-1 cells seeded on coverslips were treated with PMA for 48 h and then infected in the absence or presence of IFN-λ3. After 24 h post-infection (pi), cells were washed with PBS to remove free parasites, fixed with 4% paraformaldehyde, and then stained with DAPI (50 µg/mL) for 30 min. After PBS wash, cells were mounted on a prolong TM gold antifade reagent with DAPI and visualized under a confocal microscope (A1R Confocal Microscope System, Nikon). For fluorescence microscopy, *L. donovani* parasites were labeled with 1 mM of CFSE-Cell Labeling stain for 30 min and then washed with PBS three times to remove excess stain. The macrophage-like cells, differentiated from THP-1 cells as above, were infected with live or heat-killed (65°C for 45 min) parasites at an MOI of 1:10 in the absence or presence of IFN-λ3 for 24 h. Then, cells were washed and fixed as above and then stained with DAPI (100 µg/mL) and 1× Phalloidin-iFluor 647 reagent for 30 min. After PBS wash, cells were mounted on a prolong TM gold antifade reagent and visualized under a fluorescence microscope (Leica DMi8 TL microscope). For light microscopy, RAW264.7 (2.5×10^5/mL) cells were grown on coverslips. After 24 h, the medium was replaced with fresh medium with or without *L. donovani* at MOI 1:20. After 24 h pi, cells were processed as above and stained with Giemsa stain. After PBS wash to remove excess stain, cells were mounted on dibutylphthalate polystyrene xylene (DPX) and visualized under BX51 (upright microscope from Olympus, Japan) with the DP 25 RGB (color) camera model (Olympus).

Measurement of cellular reactive oxygen species

Reactive oxygen species (ROS) levels were measured by two assays: the nitroblue tetrazolium (NBT) reduction assay (in THP-1-derived cells) and the DCFDA fluorescence-based assay (in RAW264.7 cells). For the NBT assay (23), after discarding media, cells were treated with 0.2% NBT. NBT was reduced by ROS to a dark-blue, insoluble form of NBT called formazan. After 3 h, NBT was discarded, and cells were treated with 50% acetic acid. After 30 minutes, OD at 570 nm was recorded (23). For the DCFDA assay, cells were grown for 24 h in clear bottom white 96-well plates, and recombinant mIFN-λ3 at different concentrations with or without NAC (100 mM concentration) was added or not into the medium; lipopolysaccharides (LPS, 1 µg/mL) was added as a positive control. After incubation of the cells for 2 h, they were stained with 10 µM DCFDA for 30 min. After washing the cells three times with PBS, they were imaged under a fluorescence microscope (Leica DMi8 TL microscope). The fluorescence intensity was measured in a live cell imager (EnSight multimode plate reader; PerkinElmer) using the Kaleido data acquisition and analysis program.

Phagocytosis assay

THP-1 (5×10^5/mL) cells were seeded on coverslips into 24-well plates and differentiated into macrophage-like cells. Zymosan was added to the cells in the absence or presence of IFN-λ3 and incubated for 24 h as per the manufacturer's (Phagocytosis Assay Kit; Green Zymosan; Abcam) protocol. Cells were washed with PBS three times to remove free zymosan particles, fixed with 4% paraformaldehyde, and then stained with DAPI (100 µg/mL) for 30 min. Cells were processed as above and visualized under a fluorescence microscope (Leica DMi8 TL microscope).

Mice experiments and histopathology

BALB/c mice (6 weeks old) reared in a pathogen-free animal care facility at the animal house of the National Institute of Pharmaceutical Education and Research, NIPER, Kolkata, were used in the study. The mice were provided with filtered air, appropriate food supplements, water, and ample light. Animal ethical clearance approval was given (cert. no. IAEC/NIPER/2021/03/02) by the ethical committee at NIPER (registration number: 2074/GO/Re/S/19/CPCSEA). Before the experiments, *L. donovani* strain AG83 was maintained in the BALB/c mice; after 2 weeks of infection, animals were euthanized for isolating amastigotes from the spleen. These amastigotes were then transformed into promastigotes in Schneider's medium (Gibco) supplemented with 20% FBS and penicillin/streptomycin, and then the culture was maintained in M199 as mentioned above. The early-passage parasites (second), in stationary phase, were used for infecting the experimental mice. In the first experiment (mIFN-λ3 pretreatment), mice (six animals/group, all female) were weighed and injected intraperitoneally with a single dose of 4 µg/animal of mouse recombinant mIFN-λ3 protein or with 100 µL PBS. After 18 h, all mice were infected intravenously with 10 million parasites/animal. Another group of mice (four animals) did not receive any treatment or infection. After 6 weeks of infection, the mice were weighed and sacrificed in an animal BSL2 facility at NIPER. Spleen and liver organs were isolated and stored in an RNAlater solution for RNA and DNA isolation and in 4% formaldehyde for histopathology.

In the second experiment (post-infection mIFN-λ3 treatment), BALB/c mice (six animals/group, all female) were infected with parasites as above by the intraperitoneal route. After 12 weeks of infection, animals were injected intraperitoneally with two doses of mIFN-λ3 protein (2 µg/animal in each dose) or with PBS, 24 h apart. After 24 h of second-dose treatment, mice were weighed and sacrificed as above. Serum was also isolated from the blood of animals from both experiments and stored at −80°C for ELISA.

Approximately 10 mg of tissue was used for DNA isolation using the QIAamp DNA Mini Kit for parasite load estimation. RNA isolation was done with the RNAqueous-4PCR Kit, and qPCR was performed for kDNA and other gene expression measurements. Relative fold expression change was calculated using the $2^{-\Delta\Delta CT}$ with *Gapdh* as a housekeeping gene.

The formalin-fixed tissues were washed with 1× PBS and dehydrated in increasing concentrations of ethanol and xylene (SRL, India). The tissue was further embedded in paraffin (HistoCore Arcadia H, LEICA, Germany), sectioned (5 µm) using HistoCore MULTICUT (LEICA) and kept adhered to slides pre-coated with egg albumin. The slides were then deparaffinized in xylene and rehydrated in descending order with ethanol. Slides were stained with hematoxylin and eosin (Sigma-Aldrich) and mounted using DPX solution (SRL). Stained slides were examined under a light microscope (Magnus, Germany) at 40× magnification using MagVision software.

Human patient and healthy control samples, ethics, and genotyping

Forty-one VL patient sera samples archived at the Indian Institute of Chemical Biology (IICB), Kolkata, were used in the study. These patients had not received any antileishmanial drugs before sample collection. Ethics approval was given by the ethical committee on human subjects of the IICB (cert. no. IICB/IRB/2021/3). Healthy control individuals whose sera and genomic DNA were included in the study were residents of different areas of Kalyani, Nadia, and Kolkata and were recruited as part of the "IFN-λ4 in human health and disease" project; this cohort is described in detail in our recent study (24). The study was approved by the Institutional Ethics Committee (IEC) of the National Institute of Biomedical Genomics, Kalyani (cert. no. 2022/1/0018). For the VL and PKDL samples included for genetic association testing, ethical clearance was obtained from the IEC of the Institute of Post-Graduate Medical Education and Research (IPGMER, Kolkata, India). Necessary permissions for the field study were obtained from the Central Directorate of the National Centre for Vector Borne Disease Control, Ministry of Health and Family Welfare. Approval was obtained from the IEC for the recruitment of new cases and the

repurposing of archived samples collected during field visits. The demographic, disease status, and other details for the patient samples are provided as Suppl. data. Informed written consent was obtained from all patients enrolled by either the patient or a legally accepted representative. A competitive allele-specific polymerase chain reaction (KASP, LGC Genomics) was used to genotype all the 66 controls and 38 cases at the SNP rs12979860, as described in our recent report (24), following the manufacturer's instructions.

Statistical analysis

Experiments with cell lines were conducted with at least two biological replicates. Individual assays like qPCR, ELISA, etc. included two-three technical replicates for each biological replicate. The average of the technical replicates for each biological replicate was deduced; the resulting value was considered one experiment. Data are represented in the figures as mean and SD. The differences between the mean values of the data from experiments carried out in any two groups were compared for statistical significance. All the qPCR experiments involving the mice had six data points from each group coming from six individual mice (n = 6) that were used to calculate the statistical significance between the mean values of the two groups being compared. A one-tailed Student t-test was used to calculate significance at an allowed α (alpha) of 0.05. Other tests used, if any, are shown in the appropriate results section, figures, or legends.

RESULTS

IFNL3 is induced by *Leishmania donovani*

We first examined, using human THP-1-derived cells by qPCR, whether *L. donovani* infection can induce type III IFNs (Fig. S1A through C). We saw that *IFNL3* was induced by *L. donovani* infection in not only THP-1 but also another monocytic cell line, U937 (Fig. 1A). Using *IFNL3*-specific TaqMan probes (Applied Biosystems), we saw that the induction that begins around 24 h post-infection (pi) increases drastically at 36 h pi (Fig. 1B) in THP-1-derived cells. We confirmed the induction at the protein level upon *L. donovani* infection in both THP-1-derived cells and also in human peripheral blood mononuclear cells (Fig. S1D). We next used the mouse macrophage cell line RAW264.7 and infected it with the parasite and measured *Ifnl3* expression using gene-specific TaqMan probes (Applied Biosystems) and saw that, similar to human cells, there was a significant induction of *Ifnl3* (Fig. 1C). The expression of mIFN-λ3 in RAW264.7 cells was further confirmed by ELISA at two different MOI levels of the parasite (Fig. 1D) and also by performing western blot with culture supernatants (Fig. S1E).

We next focused on developing a molecular and sensitive assay to measure the parasite load in infected cells so that we could test the effect of exogenously added IFN-λ3 on parasite growth. The limiting dilution assay (25), although considered the gold standard, is cumbersome, and the manual counting method of Leishman Donovan (LD) bodies on Geimsa stained slides is not very reliable (26), while recent methods have used real-time PCR to overcome the drawbacks of earlier methods (26, 27). We used the fluorescent dye DAPI on *L. donovani* infected THP-1-derived cells, and by using confocal microscopy, we were able to count the number of amastigotes (based on staining of the parasite DNA) inside the cells reliably and with high resolution (Fig. 2A and B). Next, we standardized a qPCR assay to measure the parasite load. The *L. donovani* minicircle kDNA is extensively used in the genotyping and diagnosis of the *Leishmania* parasite (28) and also to quantify the parasite load deduced by comparing standard curves derived from qPCR data that are obtained from serially diluted parasites in culture (29). First, we performed qPCR of kDNA to quantify the number of parasites in infected cells after isolating whole DNA from infected cells (Fig. 2C; a standard curve was drawn by making an increasing dilution of the promastigotes followed by isolation of their DNA and qPCR to amplify the kDNA fragment; data not shown; the parasite count was deduced from this curve). However, we aimed to develop a more direct method where the parasite

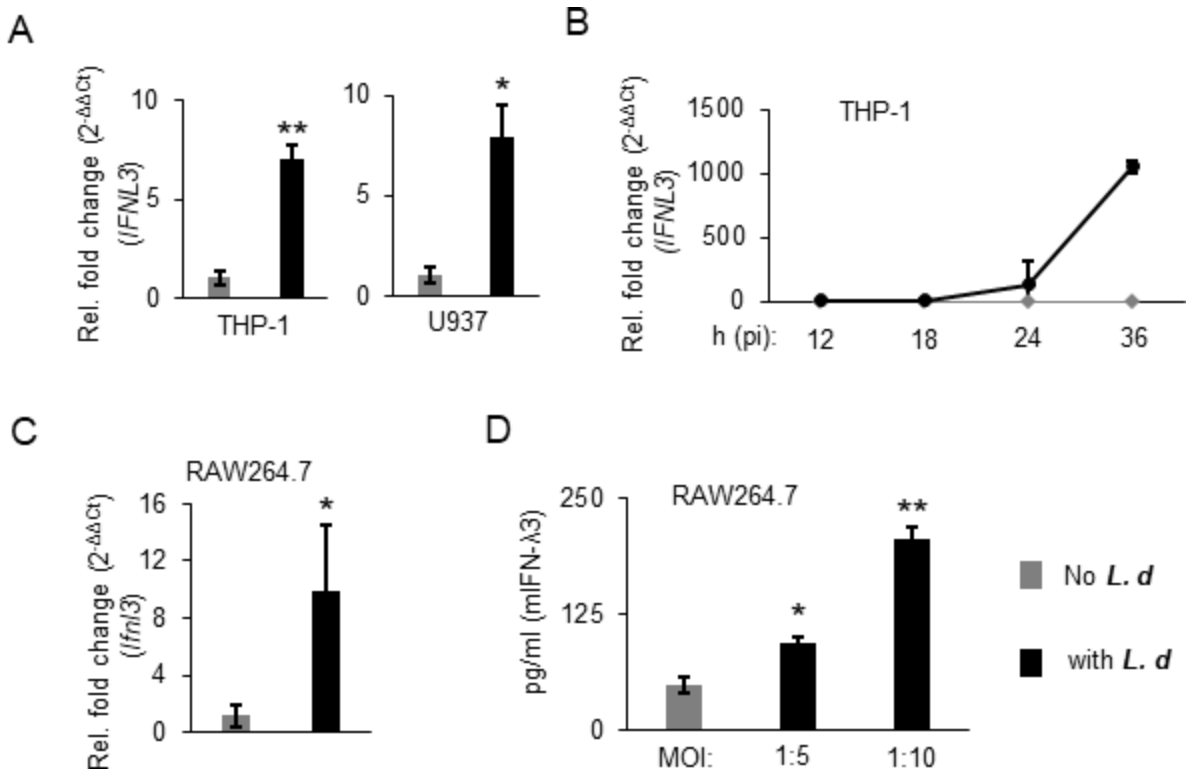

FIG 1 *L. donovani* stimulates *IFNL*3 expression. (A) Differentiated THP-1 cells or U937 cells were infected with *L. donovani* parasites for 24 h, and qPCR (using the SYBR green protocol with primers shown in Table S1) was performed to measure *IFNL3* gene expression as described in the Materials and Methods. The data are from two experiments, showing the mean and SD. *$P < 0.05$; **$P < 0.01$. (B) *IFNL3* expression was measured as in A, but using specific TaqMan primers and probes (Applied Biosystems) and at different time points after infection, as shown. The means of technical replicates are plotted with SD for each time point. pi, post-infection. (C and D) The mouse *Ifnl3* expression was measured by qPCR after *L. donovani* infection in RAW264.7 cells using gene-specific TaqMan primers and probes (Applied Biosystems) in C and by ELISA in D. The data in C are from three experiments, and the data in D are from two experiments, showing the mean and SD. *$P < 0.05$; **$P < 0.01$. *L. d, L. donovani*.

numbers could be estimated after normalizing them with a host cell gene in the qPCR assay. By using the host *GAPDH* gene as a normalizing DNA control, we were able to obtain a robust signal for the parasite kDNA in qPCR that could be used in comparative experiments (Fig. 2D). We compared the accuracy of this method with the conventional LD body counting method (Fig. 2E) in RAW264.7 cells and obtained a good correlation (Fig. 2F and G) with it. We used this method or assay throughout the study to estimate parasite load either in infected cell lines or mice and obtained reliable and consistent results. We found that it is less cumbersome than the limited dilution or the LD body staining methods.

IFN-λ3 inhibits *Leishmania donovani* growth in infected cells, and the effect is mainly mediated by ROS

We incubated cells with recombinant IFN-λ3 simultaneously with the parasite and after, 24 h, measured the parasite load using the kDNA/GAPDH method and saw that there was a significant decrease in the kDNA copies (Fig. 3A) in the IFN-λ3-treated cells [we confirmed the activity of IFN-λ3 by measuring expression of *Mx1*, an IFN-stimulated gene (ISG) in treated cells, Fig. S2A]. The effect was dose-dependent and was similar in both THP-1-derived cells and in RAW264.7 cells (using mIL28B/mIFN-λ3 in the latter). Furthermore, the effect was time-dependent: IFN-λ3 added at earlier time points after the infection, in general, had a stronger inhibitory effect on the parasite growth (Fig. 3B), again in both THP-1 and RAW264.7 cells. When we tested the effect of another type 3 IFN, IFN-λ4, which is ~30% identical to IFN-λ3 (13), we saw that it was also inhibiting the

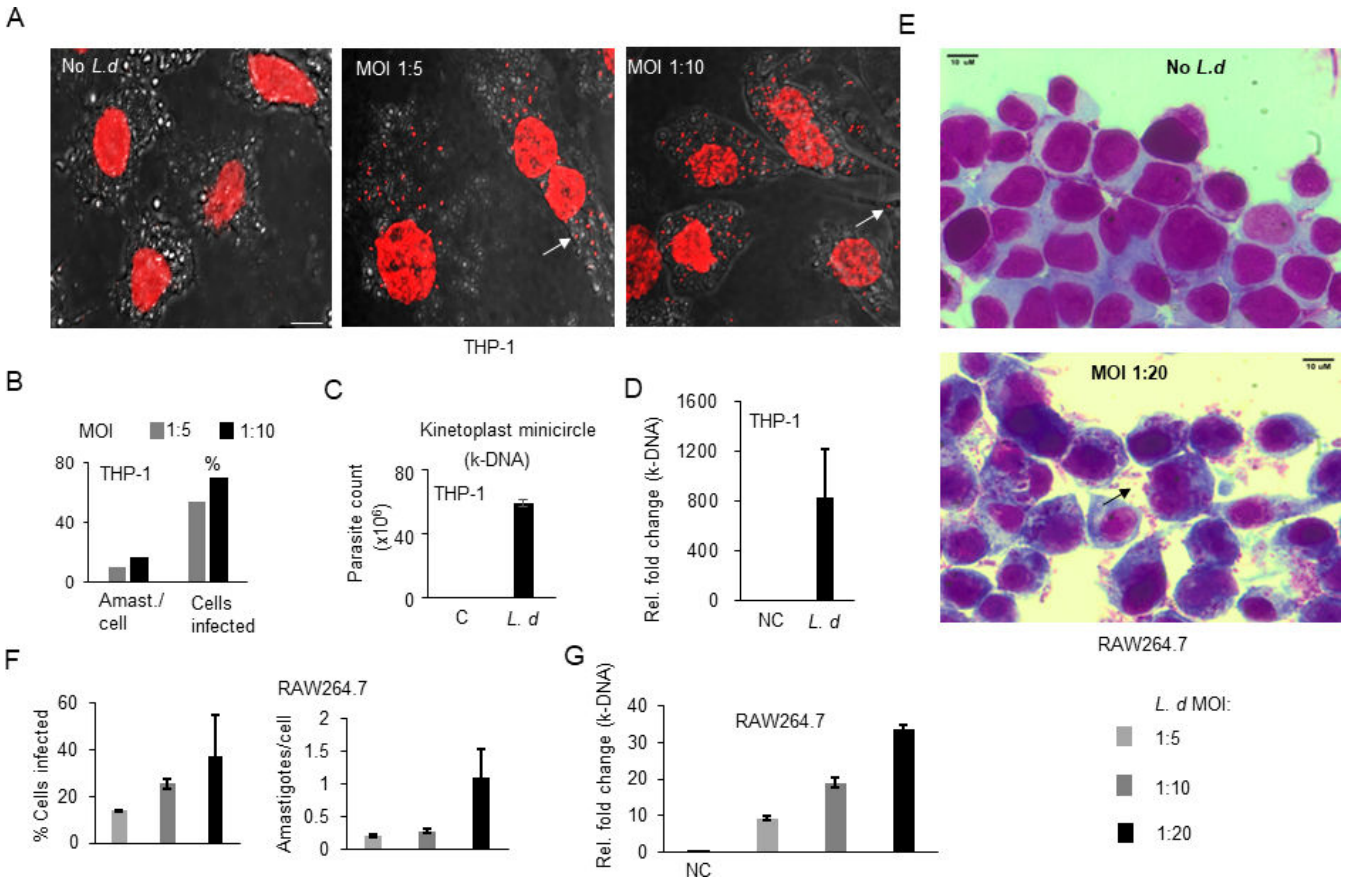

FIG 2 A microscopic and molecular assay to measure parasite load. (A) Confocal microscopy images of THP-1 cell-derived macrophage-like cells infected or not with *L. donovani* promastigotes at the MOI shown at 100× magnification. The infection was carried out for 24 h before fixing and staining. DAPI stain was used to stain both the nuclear and parasite DNA (the pseudocolor red is shown instead of the blue color of DAPI for better visualization; laser wavelength: 405.0, power: 4.3). The arrow indicates an amastigote inside a cell. Images were obtained under the DAPI channel using the NIS-Elements Imaging software (version 5.20.00). (B) The images obtained in A were manually scanned to count the number of cells infected and the number of amastigotes/cell and plotted. Then, 100–200 cells were counted per condition. (C) Parasite count in THP-1-derived cells infected with *L. donovani* (*L. d*) or not (C, control). The Ct values obtained from qPCR carried out on DNA isolated from infected cells were compared with the same represented as a standard curve obtained from qPCR carried out on promastigote DNA that was isolated from serially diluted parasite cultures in M199 medium; from this standard curve, the parasite numbers were deduced and shown as mean and SD from two experiments. (D) A new method to estimate parasite load after normalizing for host DNA concentration. The kDNA was measured from DNA isolated from infected cells by qPCR and normalized to copies of *GAPDH* DNA. The mean is shown from three separate experiments along with SD. NC, no infection control. (E) RAW264.7 cells infected with *L. donovani* were stained with Geimsa stain for LD body counting. Images were obtained in a bright field using Cell D software at 100× magnification. The arrow indicates an amastigote inside a cell. The number of amastigotes in 100 macrophage cells was counted using oil immersion lenses. (F) Data obtained from counting cells in E are plotted, showing the mean and SD. (G) Parasite load was estimated as kDNA normalized to *gapdh* from two experiments (shown as mean and SD) that were performed simultaneously with those shown in E. *L. d, L. donovani*; NC, no infection control.

parasite load in the treated cells (Fig. 3C). Next, we tested the differential effect, if any, of IFN-λ3 and IFN-λ4 on the expression of other phenotypes like cytokine secretion in the presence of *L. donovani* infection. In a recent report, we extensively characterized the molecular phenotypes in M1 and M2 macrophages differentiated in the presence of IFN-λ3 or IFN-λ4 and showed that the two IFNs can affect a large number of genes in opposite directions (22). We used M2 macrophage-like cells derived from THP-1 cells for this purpose since we have shown in this previous report (22) that IFN-λ3, compared to IFN-λ4, is more active in M2 macrophages, and also because *L. donovani* thrives in M2 macrophages (30). Both the IFNs were incubated along with the parasite in M2-macrophage-like cells for 24 h, and qPCR and ELISA were performed (Fig. 3D). Both IFNs stimulated *Mx1* but did not significantly alter the M2 macrophage marker *CD209* expression. IFN-λ3-incubated cells showed a strong and significant increase in the

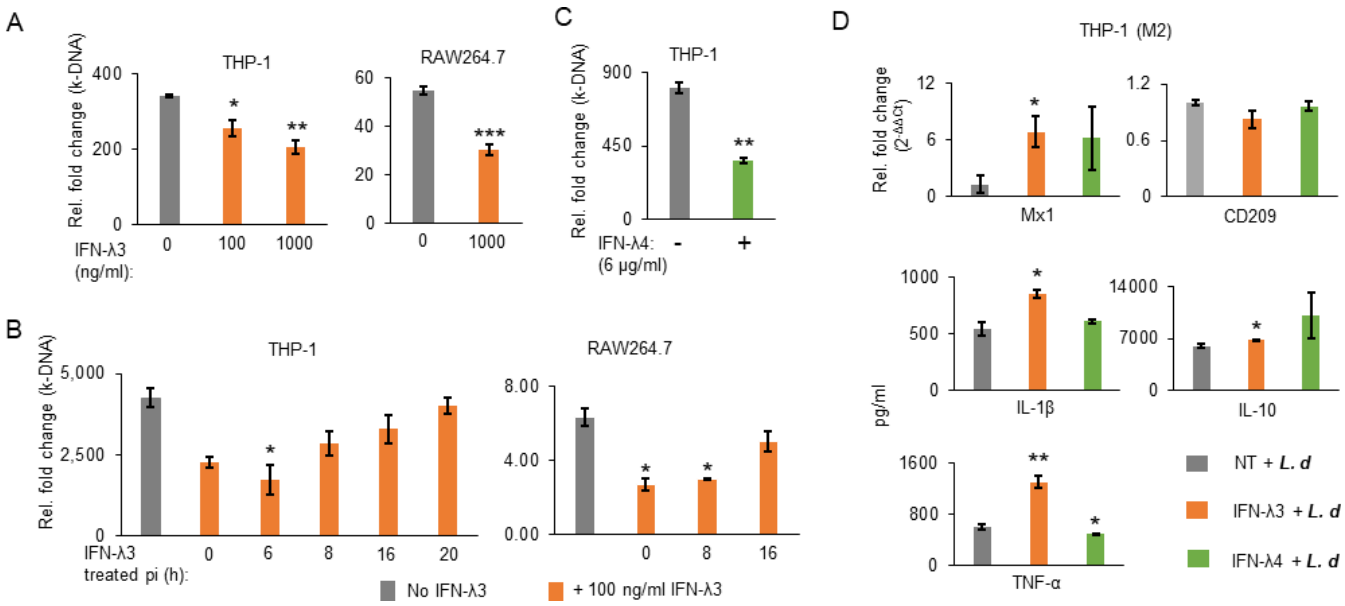

FIG 3 IFN-λ3 inhibits *L. donovani* growth in cells. (A) Human (left) or mouse(right) IFN-λ3 at the shown concentration was added along with parasites during infection, and kDNA was measured after 24 h. The data are from two experiments in THP-1-derived cells and four experiments from RAW264.7 cells, showing the mean and SD. **P* < 0.05; ***P* < 0.01; ****P* < 0.001. (B) Human (left) or mouse (right) IFN-λ3 at 100 ng/mL was added at different time points after *L. donovani* infection, and kDNA was measured after 24 h of infection. The data are from two experiments in both cell lines, shown as the mean and SD. **P* < 0.05. (C) IFN-λ4 at 6 µg/mL was added, and the experiment was as in A showing data from two experiments with mean and SD (***P* < 0.01). A high concentration of IFN-λ4 was required as the specific activity of the recombinant protein preparation is low, and 6 µg/mL would give a comparable activity to 100 ng/mL of IFN-λ3, as detailed in our previous work (16). (D) Effect of IFN-λ3 and IFN-λ4 on cytokine secretion in *L. donovani* infected M2-macrophage-like cells. M2 macrophages were differentiated for 2 days from THP-1 cells as described in our previous work (16), and IFN-λ3 at 1 µg/mL or IFN-λ4 at 6 µg/mL were added during parasite infection. After 24 h, the supernatants and cells were collected, and qPCR and ELISA were carried out. The data are from two experiments, showing the mean and SD. **P* < 0.05; ***P* < 0.01. *L. d*, *L. donovani*; NT, no treatment control.

secretion of the proinflammatory cytokines TNF-α and IL-1β and a weak but still significant increase in the secretion of the anti-inflammatory cytokine IL-10. Interestingly, in contrast to IFN-λ3, IFN-λ4 showed a significant decrease in TNF-α secretion, suggesting that, while both can inhibit the parasite *in vitro*, their effects on other immune cells may be different during *L. donovani* infections *in vivo*.

We surmised that the endogenously produced IFN-λ3 after *L. donovani* infection could also be affecting parasite growth and/or survival. In RAW264.7 cells, we saw that a significant increase in *Ifnl3* expression coincided with a significant decrease in parasite load between 24 and 36 h time-points (Fig. 4A, top). When we added a mouse IFN-λ3-specific antibody to the medium at an increasing concentration at 24 h pi and measured the k-DNA copies at 36 h pi, we saw a significant increase in parasite load in cells that got the highest antibody concentration (Fig. 4A, bottom). These results suggest that the IFN-λ3 secreted from *L. donovani*-infected cells can influence intracellular parasite survival.

To understand the mechanism of this inhibition, we measured the reactive oxygen species (ROS) in IFN-λ3-treated vs untreated cells (Fig. 4B). Using LPS as a positive control, we saw that IFN-λ3 significantly increased ROS production in THP-1-derived cells both in the absence and presence of *L. donovani* infection and at different time points after infection. We confirmed that IFN-λ3 increased ROS production in cells by using another assay (Fig. 4C). We saw that ROS production was increased by mIFN-λ3 in a dose-dependent manner in RAW264.7 cells, which could be inhibited by the ROS quencher, NAC. Next, we tested the effect of IFN-λ3 on parasite load in the presence of NAC (Fig. 4D). We added NAC at increasing concentrations (10, 50, and 100 mM) along with the parasites and IFN-λ3 to THP-1-derived macrophage-like cells and, after 24 h, measured

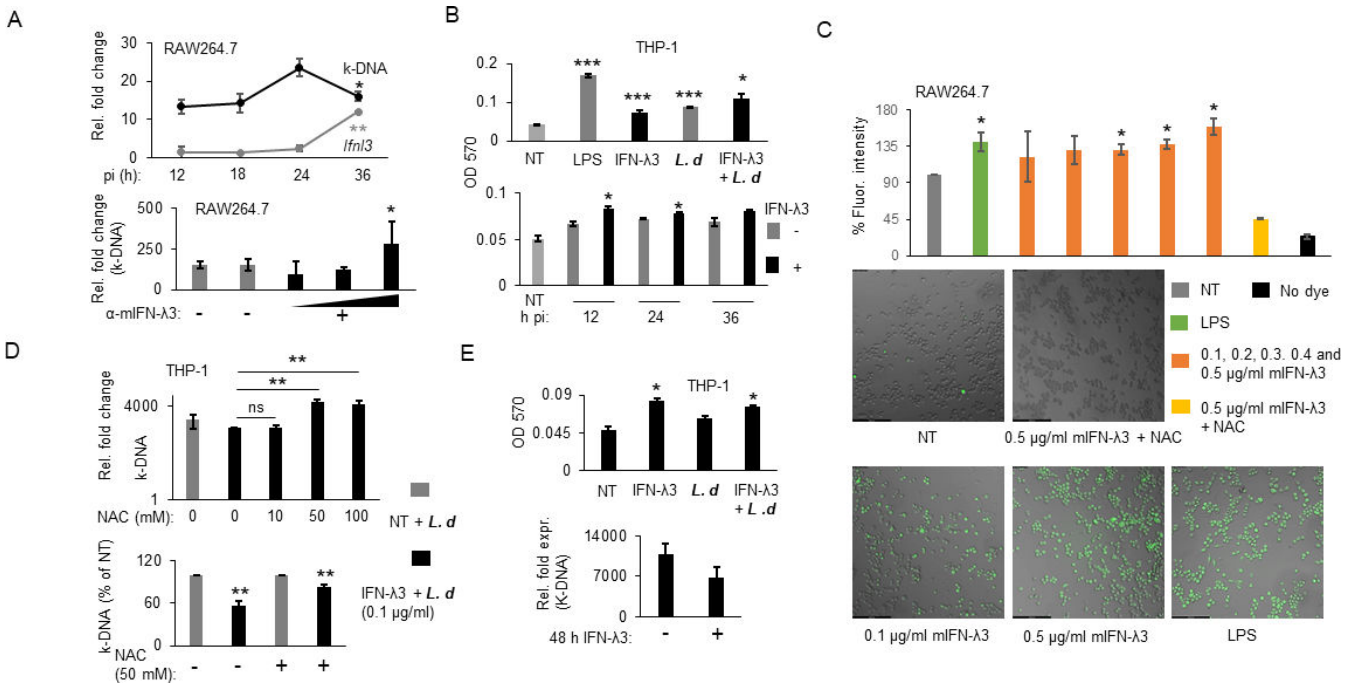

FIG 4 IFN-λ3 inhibits *L. donovani* by increasing ROS production in cells. (A) (Top) RAW264.7 cells infected with *L. donovani* for different time points as shown were subject to qPCR for kDNA (normalized to *Gapdh*) and *Ifnl3* (normalized to *Rps29*). (Bottom) Immunoneutralization of secreted mIFN-λ3 increases parasite load. The experiment was similar to the one described in the top, except that a rat anti-mouse IFN-λ3 antibody (shown as α-mIFN-λ3) was added or not at 24 h pi, at increasing concentrations as shown (1.5, 3.0, and 4.5 µg/mL) in the medium, and kDNA copies in the cells were measured after an additional 12 h (i.e., 36 h pi) of incubation. The data from both the top and bottom are from two experiments, showing the mean and SD. **P* < 0.05i, post-infection. (B) ROS levels are induced by IFN-λ3, as measured by the NBT assay. (Top) The indicated treatment (IFN-λ3, LPS, or *L. d* ± IFN-λ3) was for 2 h; IFN-λ3 was at 100 ng/mL and LPS was at 1 µg/mL. (Bottom) *L. d* infection was for indicated time points. The means from three experiments (top) and two experiments (bottom) are shown; error bars denote SD. NT, no treatment. **P* < 0.05; ***P* < 0.001; L.D, *L. donovani*. (C) mIFN-λ3 increases ROS production in RAW264.7 cells in a dose-dependent manner, as measured by a fluorescence-based assay. RAW264.7 cells were incubated with the shown concentrations of mIFN-λ3 or LPS (1 µg/mL) or NAC (100 mM) + mIFN-λ3 (0.5 µg/mL) for 2 h before staining with DCFDA. The fluorescence intensity quantified is shown at the top (data from two experiments with mean and SD are depicted; **P* < 0.05), and the bottom shows representative images taken at 20× magnification of the cells under the conditions shown. (D) IFN-λ3 can inhibit parasite load even when ROS production is inhibited. (top) *L. donovani* (*L. d*) infection was given in THP-1-derived cells as before for 24 h in the absence (NT, no treatment) or presence of IFN-λ3 and in the presence or absence of an increasing concentration of NAC added to the medium. The parasite load was estimated after 24 h pi. (Bottom) As in top, but the kDNA copies are shown after normalizing to NT and NAC at 50 mM; data are from two experiments showing the mean and SD. ***P* < 0.01. (E) (Top) THP-1 cells were pretreated with 50 ng/mL of IFN-λ3 for 48 h (incubated along with PMA), and then the media was removed and *L. donovani* (*L. d*) or mock infection (1:10 MOI) was given for 2 h. ROS levels were measured by the NBT assay. Data from two experiments with mean and SD are shown. **P* < 0.05. NT, no treatment. (Bottom) kDNA levels shown in THP-1 cells that were pretreated with 100 ng/mL IFN-λ3 or not (incubated along with PMA for 48 h) were washed off the media and infected or not with *L. donovani* for 24 h, and kDNA was measured by qPCR as before. The data are from two experiments, showing the mean and SD. Similar experiments with IFN-λ4 are shown in Fig. S2B.

the k-DNA copies. It appeared that NAC was able to relieve the inhibitory effect of IFN-λ3 at least at the higher concentrations of 50 and 100 mM, if not at 10 mM (Fig. 4D, top). We performed another experiment wherein we added NAC at 50 mM to both IFN-λ3-treated and untreated cells during parasite infection and measured the effect on k-DNA copies 24 h pi (Fig. 4D, bottom). Interestingly, we saw that even in the presence of NAC, there was significant inhibition of parasite load by IFN-λ3, even though the effect was lesser in cells where NAC was absent (Fig. 4D, bottom). These results suggest to us that IFN-λ3, in addition to inducing ROS, could be using other mechanisms to inhibit the parasite load, even though inhibition by ROS induction seems to be the major mechanism.

We checked if pretreatment (for 48 h) (before parasite infection) of THP-1 cells with IFN-λ3 could also affect ROS levels (Fig. 4E, top). We saw that ROS levels were significantly higher in pretreated cells, both in the presence and absence of the parasite. In line with these results, the parasite load at 24 h pi was lower in pretreated cells (Fig. 4E,

bottom). Similarly, we saw that IFN-λ4-pretreated cells showed significantly increased ROS levels and supported a significantly lesser parasite load after pretreatment with IFN-λ4 (Fig. S2B). These results clearly hint toward an antiparasitic effect of type 3 IFNs in *L. donovani*-infected cells, at least under *in vitro* conditions.

Next, we wanted to understand whether IFN-λ3 inhibited the uptake of the parasite or its replication or used both strategies in causing the antiparasitic effect. For this, we used fluorescence microscopy, in which we manually counted the number of cells that were infected and also the number of amastigotes per cell (Fig. 5A) in IFN-λ3-treated and untreated cells. We saw that the number of parasite-infected cells was lower in IFN-λ3-treated cells than in untreated cells; however, the number of parasites per cell was not very different. This could suggest that the uptake of promastigotes by the cells was affected by IFN-λ3, but once taken up by the cells, IFN-λ3 had a lesser role to play. To test this, we stained the promastigotes with CFSE stain, and before infection, we heat-killed them at 65°C for 45 min (and confirmed that they did not replicate inside the cells, not shown) and incubated them with THP-1-derived macrophage-like cells in the presence and absence of IFN-λ3. After 24 h, we observed under a fluorescent microscope and manually counted the number of cells that showed the presence of the parasite and also the number of parasites per cell (Fig. 5B). Interestingly, we did not see any major differences between the IFN-λ3-treated and untreated cells, suggesting that the phagocytosis ability of the cells was not affected by IFN-λ3. We confirmed this by using another fluorescent antigen (zymosan, a fungal product), whose uptake by the macrophage-like cells was not significantly affected even at high concentrations of IFN-λ3 (Fig. 5C). These results indicate that even though the phagocytic ability of the cells is not affected by IFN-λ3, some other early event in the parasite intake (like phagosome or phagolysosome maturation) may have been affected by it, which led to a lesser number of cells harboring the parasite after 24 h of infection (Fig. 3 to 4) in the treated cells.

To understand this better, we designed an experiment with several strategies wherein IFN-λ3 was added at different time points during infection, where infection was given for a limited time, and when infection was allowed for 24, 48, or 72 h (Fig. 5D). In the experiments described thus far, we have used a continuous infection condition at 1:10 MOI, wherein the promastigotes were allowed to infect the cells for the entire 24-h duration of incubation. In the new design, we gave infection at 1:20 MOI, but only for 6 h, after which the uninfected parasites were removed by rigorous washing (strategy I, Fig. 5D). This limited infection strategy allowed us to add IFN-λ3 at different stages to understand its specific effects on uptake and/or replication/growth of the parasite. We either added IFN-λ3 along with the parasites (strategy II), immediately after the removal of uninfected parasites (strategy III), or both during infection and soon after the removal of uninfected parasites (strategy IV). In strategy V, we added IFN-λ3 at 24 h, before which a 6-h infection was given as in strategy I, and measured kDNA at 48 h pi (Fig. 5D). We also had experiments under the continuous infection strategy with 1:10 MOI, as before, but with 24-, 48-, and 72-h incubation periods.

The results showed that the parasite load increased over time beyond the 24-h pi time-point (Fig. S2C and D), but the time-point of increase was also dependent on whether the infection was continuous or limited. Under the continuous infection strategy (MOI 1: 10), there was a highly significant increase in parasite load between 48 and 72 h pi time-points (Fig. S2C). While under limited infection conditions (MOI 1: 20), there was a highly significant increase in the parasite load between 24 and 48 h pi, but later showed a decrease by 72 h pi (Fig. S2D). This suggested that, under limited infection conditions, the intracellular host response was able to regulate parasite growth and/or survival inside the cells between 48 and 72 h pi time-points. To understand the effect of exogenously added IFN-λ3 on the parasite load, we normalized the parasite load data from IFN-λ3-treated samples with that from the no treatment control samples in both the continuous, and limited infection strategies and the results are presented in Fig. 5E.

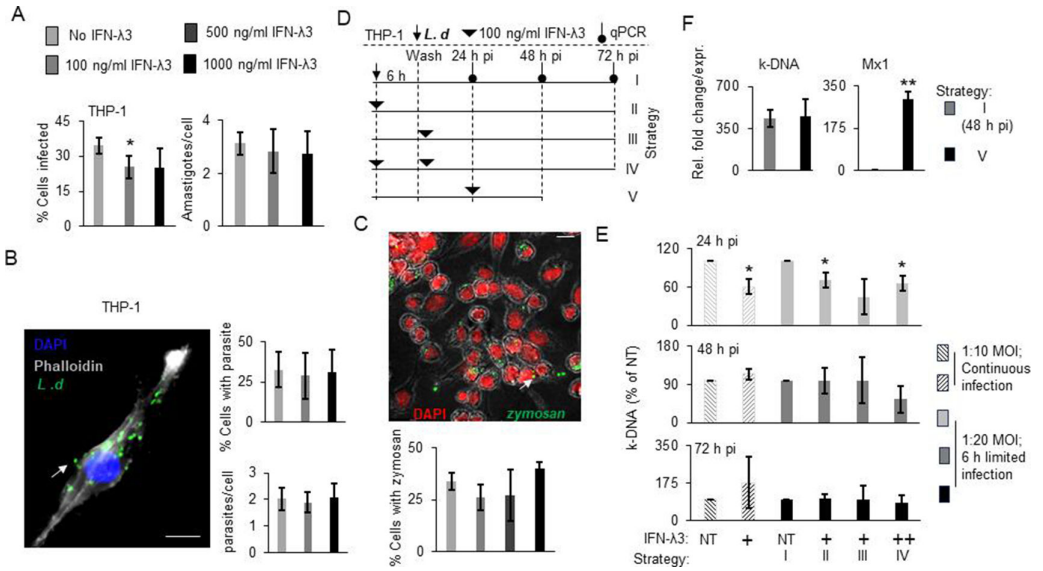

FIG 5 IFN-λ3 targets an early event in parasite uptake. (A) IFN-λ3 at the indicated doses (the color key for the doses shown is the same for A, B, and C) were incubated along with the promastigotes, and slides were stained with DAPI, and the amastigotes presence and numbers were manually counted. The data are from three (for no treatment) and four (for IFN-λ3 treatment) independent experiments, each with 100–200 individual cells shown as the mean and SD. **P* < 0.05. (B) (Left) Fluorescence microscope image of THP-1-derived cells incubated with CFSE-stained heat-killed *L. donovani* showing different stains. The arrow indicates a parasite taken up by the cell by phagocytosis. (Right) Manual counting of the parasite inside the cells and numbers was done as above and plotted. The data are from four independent experiments, each involving 100 to 200 individual cells, showing the mean and SD. For B and C, live parasites inside the cells were observed with the DAPI channel, while heat-killed parasites were observed under the GFP channel. Images were obtained under DAPI (imparts red pseudocolor), GFP (green), and Texas Red (imparts gray pseudocolor). (C) (Top) Fluorescence microscopic image of THP-1-derived macrophage-like cells that have taken up zymosan in a phagocytosis assay as described in the Materials and Methods; images were obtained under DAPI (imparts red pseudocolor), GFP (green), and Brightfield. The arrow indicates zymosan inside a cell. (Bottom) Manual counting of the cells with zymosan was performed as in B and plotted. The data are from two separate experiments with ~250 cells in each, showing the mean and SD. For B and C, image analysis was done using Leica Application Suite X software (version 3.7.2.22383) at 100× magnification. (D) Schematic representation of an experimental design with five (I-V) strategies. *L donovani* (*L. d*) infection (downward arrow) was given at 1:20 MOI for only 6 h, after which the uninfected promastigotes were removed after rigorous washing with PBS. IFN-λ3 treatment (inverted dark triangle) was given at the depicted time points, and after the indicated incubation periods, cells were collected and quantified for kDNA copies by qPCR (downward arrow with round head). (E and F). IFN-λ3 targets an early event during parasite uptake. Experiments as designed in the schematic representation shown in D were carried out, and results are presented in E (strategies I-IV) for 24 (E, top), 48 (E, middle), or 72 h pi (E, bottom) and F (strategies I for 48 h pi and V). 1:10 MOI and continuous infection conditions as described for previous experiments were also carried out, but the incubation periods included 48 and 72 h pi along with 24 h pi (shown in E middle, bottom, and top, respectively). qPCR was performed to estimate kDNA copies and ISG expression. The kDNA copies were normalized to NT (no IFN-λ3 treatment) and shown in E, while the actual fold changes are shown in F. The data in both E and F are from two experiments showing the mean and SD. **P* < 0.05; ***P* < 0.01. The data shown in E are also shown with actual fold changes and without normalization to NT control samples in Fig. S2E and F.

Under the continuous infection strategy and 1:10 MOI, as shown earlier, IFN-λ3 inhibited the parasite load that was measured after 24 h (Fig. 5E, top). However, the effect was lost if the same cells were incubated for 48 or 72 h pi (Fig. 5E, middle and bottom; Fig. S2E). The parasites in the IFN-λ3-treated cells that were lagging behind at 24 h pi had caught up (or even overtaken, Fig. S2E) with their counterparts in the IFN-λ3-untreated cells in 2-3 days after infection. This indicates that the effect of IFN-λ3 is only transient and that it is unlikely to target the parasites directly (as opposed to a host pathway) since the parasites show complete recovery if they are allowed for longer durations to grow (Fig. S2E). Next, the limited infection strategy II showed that a 6-h presence of IFN-λ3 in

the media during infection was sufficient to reduce the parasite load measured after 24 h of infection (Fig. 5E, top). Interestingly, addition of IFN-λ3 immediately after removal of the uninfected parasites showed an inhibitory effect on parasite load after 24 h pi (strategy III; Fig. 5E, top). This agrees with the results from Fig. 5A through C, which suggested that IFN-λ3 may not be affecting phagocytosis. This is because, in strategy III, IFN-λ3 was added after the parasites were internalized, but it still was able to inhibit parasite load at 24 h pi, confirming our hypothesis that an early event of parasite uptake, not necessarily phagocytosis, is being affected by IFN-λ3. Strategy IV for 24 h showed that an additional dose after removal of uninfected promastigotes along with the one during internalization did not significantly increase the inhibitory effect of IFN-λ3 (Fig. 5E, top), suggesting that there may be a narrow window during the initial phase of the parasite uptake that IFN-λ3 could be targeting and that this window overlaps with either of the time points that we chose for the addition of IFN-λ3. This is because, had the window been larger, we would have seen an additive or synergistic effect of the two doses of IFN-λ3. When infection was allowed under all four strategies for 48 and 72 h, interesting results were observed (Fig. 5E, middle and bottom). First, at 48 h pi, IFN-λ3 had no effect on the parasite load either when it was added during internalization (strategy II) or soon after it (strategy III), as there was no significant reduction of the parasite load seen on an average from two independent experiments (Fig. 5E, middle; Fig. S2F). However, in slight contrast to conclusions we drew from results that we saw at 24 h pi, IFN-λ3 given as two doses under strategy IV was still able to show its inhibitory effect on the parasite load measured after 48 h pi (Fig. 5E middle; Fig. S2F), suggesting that the parasites that got a stronger effect of IFN-λ3 due to the two doses given in a short interval could not overcome the inhibitory effect compared to those that received a single dose, since they were struggling to catch up with the untreated samples or with samples that received a single dose under strategies II and III (Fig. 5E middle; Fig. S2F). Nonetheless, they were able to overcome the inhibition if they were allowed to grow for an additional 24 h (i.e., 72 h pi) (Fig. 5E, bottom; Fig. S2F). At 72 h pi, all three strategies II, III, and IV failed to show any significant inhibition by IFN-λ3 on the parasite load (Fig. 5E, bottom; Fig. S2F). These results indicate that: (i) an early event during parasite uptake is targeted by IFN-λ3, and (ii) the effect of IFN-λ3 is only transient and the parasites can overcome the effect at later time points. To conclusively answer the question of whether IFN-λ3 affects parasite replication or survival once the parasite is inside the cells, we carried out experiments in strategy V, where IFN-λ3 was added at 24 h pi and parasite load was estimated at 48 pi (schematic representation in Fig. 5D). By 48 h pi, the promastigotes would have converted to amastigotes and be actively dividing (31), since we saw that there was an ~4.5-fold increase in parasite load between 24 and 48 h pi in the no treatment strategy (strategy I) (Fig. S2F). The results clearly showed that IFN-λ3 had no effect on parasite replication or survival when added after 24 h of infection, even though it showed high ISG induction (Fig. 5F).

In summary, our results thus far indicate that IFN-λ3 can inhibit *L. donovani* by targeting an early event in parasite uptake but may not have a sustained effect of inhibition on the parasite. Furthermore, the effect is mediated mainly by the induction of ROS but could involve other mechanisms, including the secretion of proinflammatory cytokines (Fig. 3D). The mouse model would be ideal to test the hypothesis that IFN-λ3 can act as a drug against *L. donovani,* based on the results we have obtained thus far in cell line models.

IFN-λ3 treatment in mice infected with *Leishmania donovani* fails to inhibit parasite growth, even though it mediates pathological changes in the liver

We used the BALB/c mouse model as it readily supports robust *L.donovani* infection due to a lack of M1 macrophage polarization (7). We performed two experiments to test the potential antiparasitic effect of IFN-λ3. First, we pretreated mice (n = 6 per group) intraperitoneally with either PBS or 4 µg/animal of mouse IL28B/IFN-λ3 (R&D Systems) for 18 h. We infected these pretreated mice intravenously with 10 million promastigotes of

L. donovani and allowed the infection for 6 weeks, then sacrificed them. In the second experiment, we infected the mice (n = 6 per group) with *L. donovani* intraperitoneally as above for 12 weeks and then treated with PBS or 4 µg/mouse of mIL28B/mIFN-λ3 in two doses (2 µg each) 24 h apart; the animals were sacrificed 24 h after the second dose.

We saw that there was an increase in *Ifnl3* expression in the spleen of *L. donovani* infected mice (n = 6) compared to uninfected control mice (n = 4), even though it was not significant (Fig. S3A); on the other hand, the *Ifnl3* expression in the liver was completely absent both in infected and uninfected animals. We next measured and compared by qPCR, along with the parasite kDNA, the expression of nine different genes in the liver and spleen of the animals belonging to the first experimental group (i.e., the mIL28B/IFN-λ3 pretreated group) (Fig. 6). First, there was no difference in the parasite load between the treated and untreated animals in either the liver or spleen. Second, there were some genes that showed different levels of expression between the treated and untreated groups, but except for *Il4* in the spleen and *Arg1* in the liver, the difference was not statistically significant (Fig. 6). We next looked at the histopathological changes in the liver associated with mIl28B/mIFN-λ3-treated vs untreated animals (Fig. 7A and B). Strikingly, we saw that *L. donovani*-infected animals that received mIl28B/mIFN-λ3 pretreatment had developed several changes associated with inflammation in their livers (Fig. 7A) (e.g., ballooning degeneration, which is characteristic of nonalcoholic steatohepatitis in humans). Similarly, we saw pathological changes associated with the spleen of the pretreated group as well (Fig. S3B). These results indicate that even though the mIl28B/mIFN-λ3 pretreatment failed to reduce the parasite load as expected from *in vitro* results (Fig. 3), there were definitely pathological changes associated with the treatment in the context of *L. donovani* infection, especially in the liver. We also looked at serum IFN-γ, IL-4, and IL-10 in these mice and saw that the animals that received the mIFN-λ3 treatment had an increased IL-10 level that was marginally significant (P = 0.06; Fig. 7C).

In the second experimental group (i.e., mIl28Bm/IFN-λ3 treatment after 12 weeks of *L. donovani* infection), we saw that there was a significant increase in the size of the spleen (splenomegaly) of the animals that received the two-dose mIl28B/mIFN-λ3 treatment (Fig. 8A). Interestingly, contrary to expectation from our *in vitro* results (Fig. 3 to 5), instead of a decrease in the parasite load, we saw a strong trend toward its increase in the spleens of the treatment group; concomitantly, the spleens from the treatment group had better lymphocyte proliferation than the untreated group (Fig. S4). A similar trend for kDNA was not seen in the livers (Fig. 8A), while the pathology was also not severe in the treatment group (Fig. S4). No other changes in the expression of any of the genes tested were observed. Furthermore, there were no significant differences in the levels of serum IFN-γ, IL-4, and IL-10 in the treated vs untreated mice (Fig. 8B). These results indicate that IFN-λ3 may have a role to play in the pathology involving *L. donovani* infection, but certainly it was not inhibiting the parasite in the *in vivo* system in the conditions tested.

IFN-λ3 significantly associates with leishmaniasis in humans

VL is a fatal disease in untreated humans with symptoms of prolonged pyrexia, hepatosplenomegaly, and weight loss. PKDL, a cutaneous manifestation, is a sequel to VL, occurring in only a subset of VL-cured patients (32). We first measured the serum IFN-λ3 levels in VL patients (n = 41) and compared the same with healthy controls (n = 81) (Fig. 9A). We saw a highly significant increase in the level of IFN-λ3 in VL patient sera (Fig. 9A), in line with our results that *L. donovani* can induce *IFNL3* expression (Fig. 1). We next gathered a small cohort of VL (n = 19) and PKDL (n = 19) patients and tested their *IFNL* genotype at the single nucleotide polymorphism (SNP) rs12979860. The SNP rs12979860 closely correlates with the two functional variants that are known to regulate *IFNL3* expression, rs4803217 and rs28416813 (33) and also with the IFN-λ4-generating dinucleotide variant rs368234815 (13). We compared the allele frequencies between the cases (n = 38) and a control cohort of age- and gender-matched healthy individuals (n = 66). The genotyping results showed that the cohort was in Hardy-Weinberg equilibrium

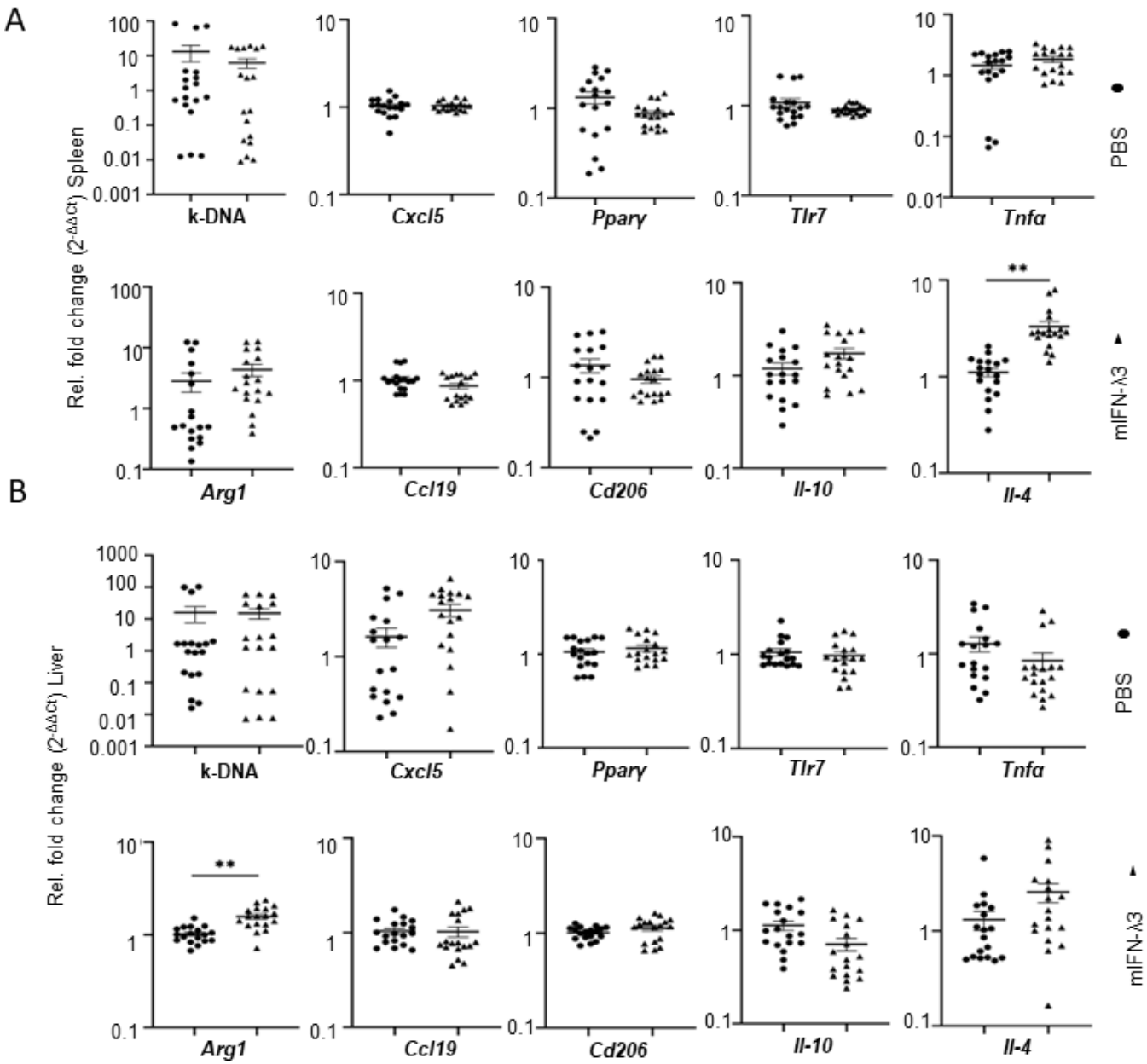

FIG 6 IFN-λ3 before infection fails to inhibit parasite load in the mouse model of VL. (A) and (B) Gene expression changes measured by qPCR from mice spleen (A) or liver (B) pretreated with 4 µg/mouse of mIFN-λ3 or PBS 18 h before infection with *L. donovani*. The infection was allowed for 6 weeks, and gene expression was quantified using primers listed in Table S1 and SYBR green (Applied Biosystems) protocol. kDNA was also measured and normalized using the $2^{-\Delta\Delta Ct}$ method. Six female mice were used in each group, and 18 data points are shown for the six samples carried out in technical triplicate. The statistical significance, however, was calculated with $n = 6$ by considering the average of the technical triplicates for each animal as the actual value for that animal. $^{**}P < 0.01$. No significant differences were observed in the body weight and organ weights for the two groups.

($P > 0.05$). Our results show that the minor allele (T) of rs12979860 that correlates with a decrease in IFN-λ3 expression (34) was significantly underrepresented in the leishmaniasis cases compared to the patient controls (Fig. 8B). The major allele is significantly associated with a risk phenotype under the recessive model (CC vs CT + TT; odds ratio = 2.13; 95% CI, 1.05, 4.57; Fisher's exact one-tailed test, $P = 0.03$). The genotype and allelic distribution were not significantly different between VL and PKDL samples (χ test; $P > 0.05$), suggesting that the association is agnostic to the VL/PKDL form of the disease (it is to be noted that all PKDL cases were VL-recovered patients; Suppl. Data). The above

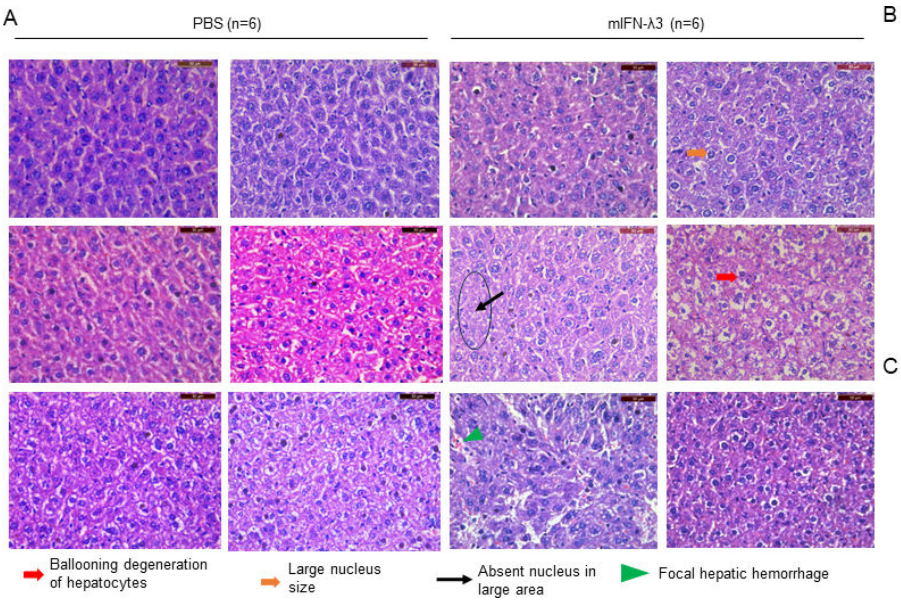

B

Histopathological alterations	Treatment	
	PBS	mIFN-λ3
Liver		
Ballooning degeneration of hepatocytes	-	++
Portal infiltration with inflammatory cells	-	+
Oval cells proliferation	+	++
Focal hepatic haemorrhage	-	+

- Nil + Mild ++ Moderate +++ High

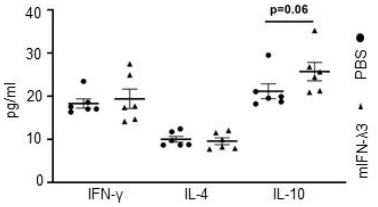

FIG 7 IFN-λ3 treatment before infection (18 h) causes distinct pathological changes in the liver of treated mice post-infection. (A) H&E-stained liver sections are shown for the 12 animals (six in each group) pretreated with PBS or 4 µg/mouse of mIFN-λ3. (B) A summary of the histopathological findings from A. Trained personnel were asked to score for each pathological feature after blinding the slide information. The data were scored first, and then the identities of the slides were revealed to the personnel, after which the summary table was made. (C) IL-10 is increased at a marginal significance level (P = 0.06) in the serum of mIFN-λ3-treated mice. The sera from mice described in Fig. 6 were subjected to ELISA for the three mouse cytokines shown.

results from human samples show that the *IFNL* locus and specifically the *IFNL3* gene may be involved in the susceptibility to and pathogenesis of leishmaniasis in humans.

DISCUSSION

Type 3 IFNs, since their discovery in 2003 and 2013 (11–13), have become an important topic of research involving not only infectious but also inflammatory diseases. They were initially thought to be redundant to their type 1 counterparts, but it is now becoming clear in light of accumulating evidence, especially from research with viruses involving the respiratory and gastrointestinal tract, that they are distinct from type 1 IFNs and have separate roles in resolving viral infections (35). They are known to protect the barriers from excessive inflammation against viral infections while still being antiviral (35). However, clarity is lacking in our understanding of the exact roles they play in infection and immunity involving different pathogens, including viruses. For instance, IFN-λ4, which is a potent antiviral cytokine *in vitro* that can inhibit diverse viruses like flaviviruses (HCV, dengue virus, and yellow fever virus) (36), human immunodeficiency virus (37), coronavirus (38) and Sendai virus (39) is paradoxically a risk factor *in vivo* in humans against HCV and some pediatric respiratory and gastrointestinal viral infections (20, 40). Similarly, a study has shown that while IFN-λ could inhibit the replication of encephalomyocarditis virus (EMCV) in *vitro*, it did not do so in the *in vivo* mouse model, while the same study showed that it inhibited other viruses like lymphocytic choriomeningitis virus (LCMV) and herpes virus (HSV) *in vivo* (41). This inconsistency is observed with bacterial pathogens too; for example, while IFN-λ reinforces epithelial barrier surfaces and shows protection against some bacteria (42), in other bacteria it seems to be a risk factor (43).

In protozoan parasite infections too, with the limited studies that have been reported, a clear picture on the protective vs risk features of IFN-λs has not emerged (19). In mice lacking the IFNL receptors, the antibody response to and clearance of *Plasmodium yoelli* is better than in wild type mice (44), while in *Cryptosporidium parvum* infection in mice, immunoneutralization of IFN-λ2/3 led to a worse outcome (45) and in another study with

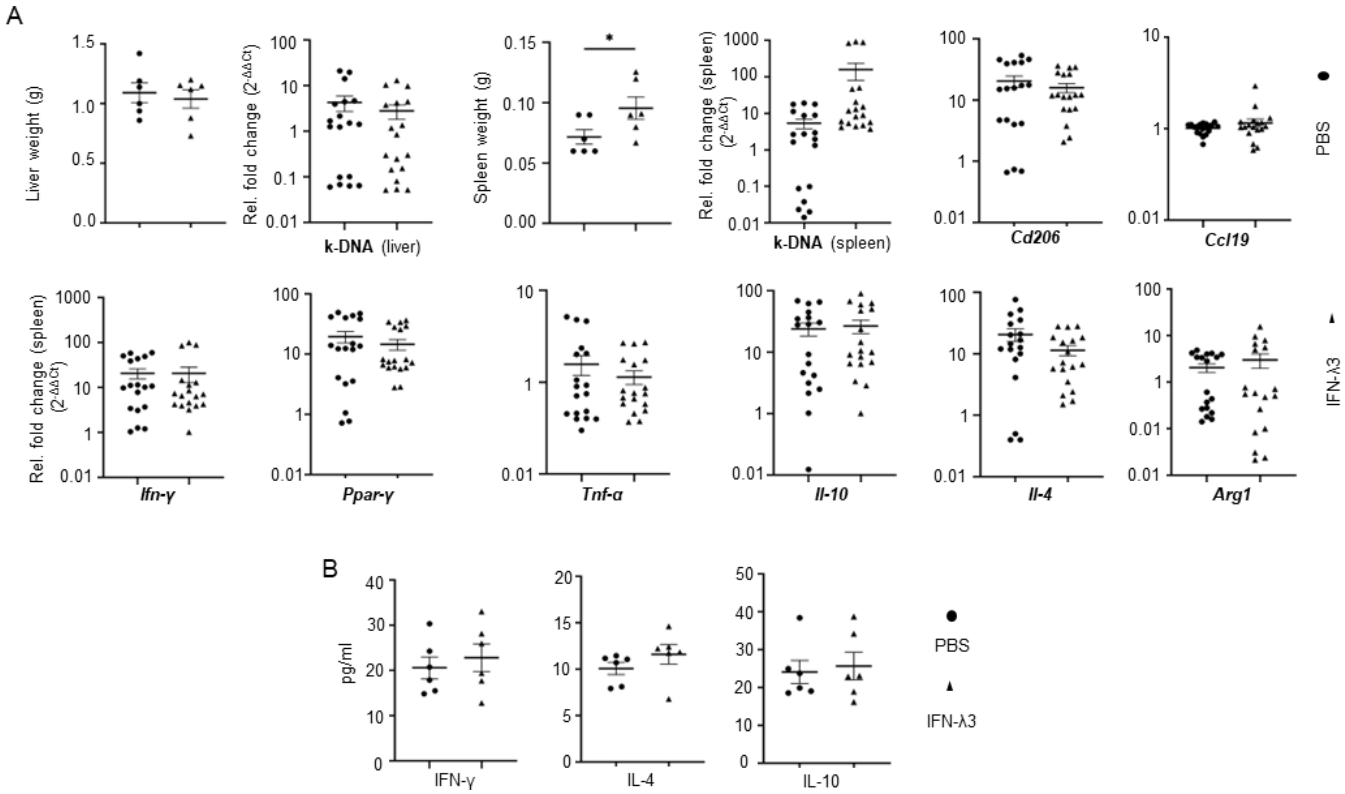

FIG 8 IFN-λ3 treatment during infection fails to inhibit parasite load in the mouse model of VL. (A) Liver and spleens of the mice treated with PBS or 4 µg/mouse of mIFN-λ3 (in two doses of 2 µg/mouse in each dose given 24 h apart) at 12 weeks of infection were collected and weighed before subjecting them to qPCR for kDNA (liver and spleen) and other genes (spleen only). Each group had six animals ($n = 6$); 18 data points are shown for the six samples carried out in technical triplicates for qPCR data. The statistical significance, however, was calculated with $n = 6$ by considering the average of the technical triplicates for each animal as the actual value for that animal; for the organ weights, single measurements were taken for each organ belonging to each animal. *$P < 0.01$. (B) The sera from mice were subjected to ELISA for the three mouse cytokines shown.

C. parvum, a protective effect of IFN-λ was seen (46). Furthermore, IFN-λ4-generating allele associated with increased risk of malaria in children (20). In this context our present study contributes to further understanding of the possible roles of type 3 IFNs in another protozoan parasite infection that causes important neglected diseases of the tropics.

Our study shows for the first time the host-pathogen interactions involving *Leishmania* and type 3 IFNs comprehensively by using both cell-based and animal models and also complements it with data from affected humans. First, we show that the parasite can induce *IFNL3/Ifnl3* expression in both human and mouse-derived macrophage cell lines (Fig. 1). Second, we show that exogenously provided IFN-λ3 can suppress parasite replication in both cell lines (Fig. 3). Third, we show in the mouse model of VL that recombinant mIFN-λ3 does not show any suppression of the parasite growth; instead, we see a trend toward an increase in the parasite load (Fig. 8A, in the spleen) with accompanying splenomegaly that was statistically significant. Fourth, we complement the data from the mouse model by showing that there is a highly significant increase in serum IFN-λ3 in VL patients (Fig. 9A); further, the T allele of the SNP rs12979860 that is associated with lower expression of IFN-λ3 in humans (33, 34) is present in a significantly higher proportion in patient controls (29%) than in VL cases (16%) (Fig. 9B). These latter results project a risk phenotype that IFN-λ3 could attribute to the host in the context of *L. donovani* infection.

We have also shown that IFN-λ4, an IFNL that is only ~30% identical to IFN-λ3 (13) can also inhibit parasite load in infected cells by inducing ROS production (Fig. 3C; Fig. S2B), even though it may not have the same effect as IFN-λ3 on cytokine secretion (Fig. 3D). The data we present in Fig. 3 and 4 clearly provide evidence that IFN-λ3 (and IFN-λ4) have

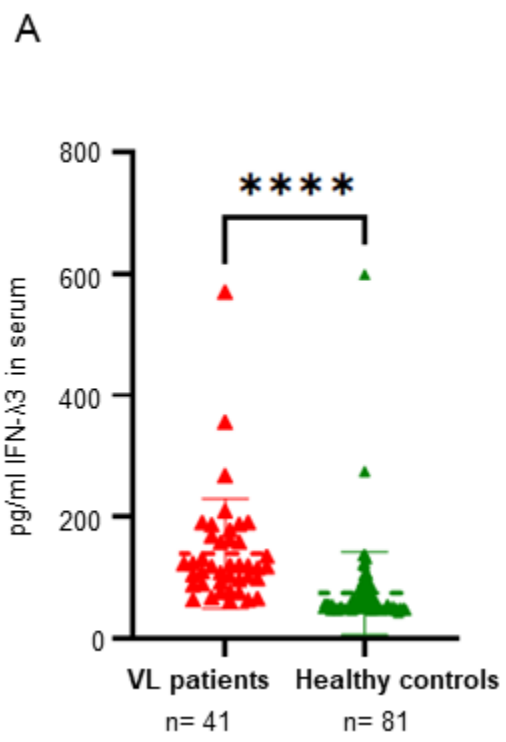

B

rs12979860 (C>T)

	Cases	Controls
VL (n, %)	19 (50)	
PKDL (n, %)	19 (50)	
Total (n, %)	38 (100)	66 (100)
CC (n, %)	27 (71)	34 (52)
CT (n, %)	10 (26)	26 (39)
TT (n, %)	1 (3)	6 (9)
HWE (p-value)	0.94	0.75
C alleles (n, %)	64 (84)	94(71)
T alleles (n, %)	12 (16*)	38 (29*)
*MAF		

Chi-square test of association for allelic model (two-tailed) p-value= **0.03;**
OR $_{T\ allele}$ = 0.46 (95% CI, 0.22, 0.95) (two-tailed); p-value= **0.04**

FIG 9 Leishmaniasis is significantly associated with IFN-λ3 in humans. (A) Serum IFN-λ3 levels in VL patients are strongly upregulated compared to patient controls. A highly significant difference is seen between the IFN-λ3 serum levels of VL patients and healthy controls. The mean and SD values for the two groups are shown: ****$P < 0.0001$. A two-sample *t*-test gave a *P*-value of 1.981×10^{-05}; however, the variances were significantly different between the two groups ($P =$ **0.02**, F-test), and the test for normality (Kolmogorov-Smirnov test) gave a highly significant *P*-value ($P < 2.2 \times 10^{-16}$), suggesting the non-normal distribution of data. Hence, we also tested the significance using the Wilcoxon rank sum test with continuity correction; this test also showed a highly significant association ($P = 1.337 \times 10^{-11}$). (B) The *IFNL* SNP rs12979860 significantly associates with leishmaniasis (both VL, visceral leishmaniasis and PKDL, post-kala-azar dermal leishmaniasis; all PKDL patients had recovered from VL) in humans; the complete details of the patients recruited for the study are given in Suppl. Data. % data are rounded off to the closest whole number; HWE, Hardy-Weinberg equilibrium; MAF, minor allele frequency; CI, confidence interval. All tests were carried out using RStudio 4.1.0.

antiparasitic properties, which prompted us to undertake the mouse studies. The results presented in Fig. 5, however, provided additional clues to the possible mechanism of inhibition, wherein we saw that IFN-λ3 may be targeting an early event inside the parasitophorous vacuole/phagolysosome. Results from Fig. 5F clearly indicated no active role for IFN-λ3 in inhibiting the parasite load once the parasites were actively dividing.

Nonetheless, we wanted to test whether IFN-λ3 could act as a "drug" against *L. donovani* in the BALB/c mouse model. We chose this model since it supports robust infection, and a drug-like effect, if any of IFN-λ3, could easily be captured in this setting, even though this may not have been the best model to study IFN-λ3-immune cell interactions, for which a resistant mouse strain like C57BL/6 would have been more appropriate. Despite our *in vitro* experiments providing strong evidence to show that IFN-λ3 could inhibit parasite load mainly by inducing ROS (Fig. 4B and C) and possibly by additional mechanisms (Fig. 4D and 3D), our mouse results did not support such a possibility. We deliberated on the possibility that since type 3 IFNs function at the barrier surfaces and since our mIFN-λ3 delivery was intraperitoneal (while the parasite itself was delivered intravenous or intraperitoneal), could the effect of IFN-λ3 be missed by the parasite? However, our own recent studies (16, 22) have shown that macrophages respond very well to IFN-λ3, and hence this could possibly not be the reason why inhibition was not seen *in vivo*. However, we feel the most interesting results from the study come from human samples (Fig. 9), where we see a strong induction of IFN-λ3 in the serum of VL patients apart from a genetic association of an important IFNL

polymorphism with leishmaniasis, even though the latter results were obtained from a small number of samples and hence need further validation. Clearly, IFN-λ3 could not be antiparasitic in humans since such induction should have reduced the parasite burden and helped clear the infections (the serum samples were from VL patients who were not treated with any antileishmanial drugs). It is not clear why IFN-λ3, which is antiparasitic in cell culture, could be a risk *in vivo*. Complex interactions between immune and non-immune cells that an *in vitro* system cannot recapitulate and that are clearly important in the *in vivo* context could be the reason for these apparent paradoxes (40). Similar conclusions have been drawn about IFN-λ2/3 in the context of EMCV, LCMV, and HSV infections in mice in an earlier report (41).

In humans, although there are a number of genetic association studies reported that implicate the IFNL locus in different infectious and inflammatory diseases due to their close linkage on chromosome 19, it is difficult to conclusively assign causality to either IFN-λ3 or IFN-λ4 even though causal variants have been defined for both (47). In this scenario, a risk phenotype attributed to the major alleles of IFNL SNPs (that associate with higher IFN-λ3 expression) (33, 34) or a protective phenotype attributed to the minor alleles (that associate with expression of IFN-λ4 and low levels of expression of IFN-λ3) (34) would both mean that IFN-λ3 is risky for a given phenotype. We found many such associations from previous findings [summarized in reference (47)]. Notable among them was HCV-related liver fibrosis (47), wherein it was shown with genetic evidence that IFN-λ3 and not IFN-λ4 were behind excessive inflammation that was responsible for liver damage in HCV infections (48), implying that IFN-λ3 could be a proinflammatory IFN-λ. However, in our recent report, where we showed that IFN-λ3 was more active in M2 than M1 macrophages, we argued that IFN-λ3's selective effect on M2 macrophages could be the reason for its association with fibrosis rather than its proinflammatory nature (22). Since, *L. donovani* also prefers M2 macrophages for its survival (30), it is possible that our observations from human samples, where we see increased IFN-λ3 levels in VL patients (Fig. 9A) and genetic association related to increased expression of IFN-λ3 (Fig. 9B) in leishmaniasis patients, are pointing toward a selective effect of IFN-λ3 on M2 macrophages that could be an important survival factor for *L. donovani* in humans. Importantly, in our recent transcriptomics analysis of human monocyte-derived M1 and M2 macrophages differentiated in the presence of IFN-λ3 or IFN-λ4, from two independent studies (16, 22) involving samples from five different individuals, we saw the leishmaniasis disease pathway consistently showing up among the most significant pathways affected (16, 22). Our present study corroborates this analysis by showing the involvement of IFN-λs with *Leishmania* infections in different model systems as well as in humans.

Our results indicate that *L. donovani* induces *IFNL3/Ifnl3* expression, both in cell lines (Fig. 1) and also in the spleen of mice (Fig. S3A), which are indicators of a mechanism the parasite may be using to take advantage of the beneficial effects of IFN-λ3 for its own survival. Even though results from Fig. 4A suggest that the endogenously secreted IFN-λ3 could have an inhibitory effect on the parasite, later results from Fig. 5, suggest that the inhibitory effect of IFN-λ3 is only transient and can be overcome at later time points (also, the conditions of infection—continuous vs limited—were different in the experiments shown in Fig. 4A and 5E F, , and therefore we do not see any contradictions in the results). Therefore, it is possible that *L. donovani* induces IFN-λ3, which, despite its inhibitory nature, could benefit the parasite at later stages through yet unknown mechanisms. A recent report, using data from both VL patients and mouse models, showed that type I IFNs are responsible for suppressing antiparasitic immunity by increasing IL-10 production from $CD4^+$ T cells (49). Our results are in concurrence with this report, even though further research is required to identify the key players involved that can explain the seemingly contradictory nature of IFN-λ3 in *in vitro* vs *in vivo* conditions involving *L. donovani* infections. It will also be interesting to identify the pattern recognition receptors in the host (50) and the specific molecular patterns in the parasite that are engaged in inducing type 3 IFNs. This will not only help us understand

the host-pathogen interactions better but may also lead us to develop specific small-molecule inhibitors that can disrupt this interaction and negate the seemingly beneficial effect of IFN-λ3 on the parasite.

ACKNOWLEDGMENTS

M.D. thanks DBT/Wellcome Trust India Alliance (under the intermediate fellowship scheme awarded to S.C.) for salary support; S.K. thanks NIBMG; D.G.R. thanks DST INSPIRE; and S.B. thanks DBT for fellowship support. S.C. thanks the Director, NIBMG, for intramural funds, support, and encouragement for this work. This work was supported by NIBMG intramural funding to S.C.

AUTHOR AFFILIATIONS

[1]National Institute of Biomedical Genomics, Kalyani, West Bengal, India
[2]National Institute of Pharmaceutical Education and Research, Kolkata, West Bengal, India
[3]Centre for High Impact Neuroscience and Translational Applications (CHINTA), TCG-Centres for Research and Education in Science and Technology, Kolkata, West Bengal, India
[4]Regional Centre for Biotechnology, Faridabad, India
[5]Department of Pharmacology, Institute of Post-Graduate Medical Education and Research, Kolkata, India
[6]Infectious Diseases and Immunology Division, CSIR-Indian Institute of Chemical Biology, Kolkata, India
[7]Fischell Department of Bioengineering, A. James Clark School of Engineering, University of Maryland, College Park, MD, USA

AUTHOR ORCIDs

Nahid Ali https://orcid.org/0000-0002-6166-3778
Sreedhar Chinnaswamy http://orcid.org/0000-0003-0095-3453

FUNDING

Funder	Grant(s)	Author(s)
National Institute of Biomedical Genomics (NIBMG)	Intramural 60103	Sreedhar Chinnaswamy

AUTHOR CONTRIBUTIONS

Manjarika De, Formal analysis, Investigation, Methodology, Project administration, Resources, Validation, Visualization, Writing – review and editing | Soumi Sukla, Investigation, Methodology, Resources, Visualization, Writing – review and editing | Seema Bharatiya, Formal analysis, Methodology, Resources, Visualization, Writing – review and editing | Sagar Keshri, Formal analysis, Methodology, Resources, Visualization, Writing – review and editing | Debarati Guha Roy, Data curation, Formal analysis, Methodology, Resources, Writing – review and editing | Debrupa Dutta, Investigation, Methodology, Writing – review and editing | Shriya Saha, Formal analysis, Investigation, Methodology, Writing – review and editing | Sarfaraz Ahmad Ejazi, Investigation, Resources | V. Ravichandiran, Conceptualization, Project administration, Resources | Nahid Ali, Conceptualization, Resources, Writing – review and editing | Mitali Chatterjee, Conceptualization, Resources, Writing – review and editing | Sreedhar Chinnaswamy, Conceptualization, Data curation, Formal analysis, Funding acquisition, Investigation, Project administration, Resources, Supervision, Writing – original draft, Writing – review and editing.

ADDITIONAL FILES

The following material is available online.

Supplemental Material

Supplemental figures (IAI00504-23-s0001.pdf). Figures S1 to S4.
Supplemental material (IAI00504-23-s0002.docx). Table 1, primers; supplemental methods.

REFERENCES

1. Torres-Guerrero E, Quintanilla-Cedillo MR, Ruiz-Esmenjaud J, Arenas R. 2017. Leishmaniasis: a review. F1000Res 6:750. https://doi.org/10.12688/f1000research.11120.1
2. Muniaraj M. 2014. The lost hope of elimination of kala-Azar (visceral Leishmaniasis) by 2010 and cyclic occurrence of its outbreak in India, blame falls on vector control practices or co-infection with human immunodeficiency virus or therapeutic modalities? Trop Parasitol 4:10–19. https://doi.org/10.4103/2229-5070.129143
3. Regli IB, Passelli K, Hurrell BP, Tacchini-Cottier F. 2017. Survival mechanisms used by some leishmania species to escape neutrophil killing. Front Immunol 8:1558. https://doi.org/10.3389/fimmu.2017.01558
4. Liu D, Uzonna JE. 2012. The early interaction of leishmania with macrophages and dendritic cells and its influence on the host immune response. Front Cell Infect Microbiol 2:83. https://doi.org/10.3389/fcimb.2012.00083
5. Loría-Cervera EN, Andrade-Narváez FJ. 2014. Animal models for the study of leishmaniasis immunology. Rev Inst Med Trop Sao Paulo 56:1–11. https://doi.org/10.1590/S0036-46652014000100001
6. Loeuillet C, Bañuls A-L, Hide M. 2016. Study of leishmania pathogenesis in mice: experimental considerations. Parasit Vectors 9:144. https://doi.org/10.1186/s13071-016-1413-9
7. Restrepo CM, Llanes A, Herrera L, Ellis E, Lleonart R, Fernández PL. 2021. Gene expression patterns associated with leishmania panamensis infection in macrophages from BALB/C and C57Bl/6 mice. PLoS Negl Trop Dis 15:e0009225. https://doi.org/10.1371/journal.pntd.0009225
8. Beattie L, Peltan A, Maroof A, Kirby A, Brown N, Coles M, Smith DF, Kaye PM. 2010. Dynamic imaging of experimental *Leishmania donovani*-induced hepatic granulomas detects kupffer cell-restricted antigen presentation to antigen-specific CD8+ T cells. PLoS Pathog 6:e1000805. https://doi.org/10.1371/journal.ppat.1000805
9. Blackwell JM, Fakiola M, Ibrahim ME, Jamieson SE, Jeronimo SB, Miller EN, Mishra A, Mohamed HS, Peacock CS, Raju M, Sundar S, Wilson ME. 2009. Genetics and visceral leishmaniasis: of mice and man. Parasite Immunol 31:254–266. https://doi.org/10.1111/j.1365-3024.2009.01102.x
10. Fakiola M, Strange A, Cordell HJ, Miller EN, Pirinen M, Su Z, Mishra A, Mehrotra S, Monteiro GR, Band G, et al. 2013. Common variants in the HLA-DRB1–HLA-DQA1 HLA class II region are associated with susceptibility to visceral leishmaniasis. Nat Genet 45:208–213. https://doi.org/10.1038/ng.2518
11. Kotenko SV, Gallagher G, Baurin VV, Lewis-Antes A, Shen M, Shah NK, Langer JA, Sheikh F, Dickensheets H, Donnelly RP. 2003. IFN-λs mediate antiviral protection through a distinct class II cytokine receptor complex. Nat Immunol 4:69–77. https://doi.org/10.1038/ni875
12. Sheppard P, Kindsvogel W, Xu W, Henderson K, Schlutsmeyer S, Whitmore TE, Kuestner R, Garrigues U, Birks C, Roraback J, et al. 2003. IL-28, IL-29 and their class II cytokine receptor IL-28R. Nat Immunol 4:63–68. https://doi.org/10.1038/ni873
13. Prokunina-Olsson L, Muchmore B, Tang W, Pfeiffer RM, Park H, Dickensheets H, Hergott D, Porter-Gill P, Mumy A, Kohaar I, Chen S, Brand N, Tarway M, Liu L, Sheikh F, Astemborski J, Bonkovsky HL, Edlin BR, Howell CD, Morgan TR, Thomas DL, Rehermann B, Donnelly RP, O'Brien TR. 2013. A variant upstream of IFNL3 (Il28B) creating a new interferon gene IFNL4 is associated with impaired clearance of hepatitis C virus. Nat Genet 45:164–171. https://doi.org/10.1038/ng.2521
14. Kotenko SV. 2011. IFN-λs. Curr Opin Immunol 23:583–590. https://doi.org/10.1016/j.coi.2011.07.007
15. Wack A, Terczyńska-Dyla E, Hartmann R. 2015. Guarding the frontiers: the biology of type III interferons. Nat Immunol 16:802–809. https://doi.org/10.1038/ni.3212
16. De M, Bhushan A, Chinnaswamy S. 2021. Monocytes differentiated into macrophages and dendritic cells in the presence of human IFN-λ3 or IFN-λ4 show distinct phenotypes. J Leukoc Biol 110:357–374. https://doi.org/10.1002/JLB.3A0120-001RRR
17. Johnson D, Carbonetti N. 2023. Roles and effects of interferon lambda signaling in the context of bacterial infections. J Interferon Cytokine Res 43:363–369. https://doi.org/10.1089/jir.2023.0037
18. Espinosa V, Dutta O, McElrath C, Du P, Chang Y-J, Cicciarelli B, Pitler A, Whitehead I, Obar JJ, Durbin JE, Kotenko SV, Rivera A. 2017. Type III interferon is a critical regulator of innate antifungal immunity. Sci Immunol 2:eaan5357. https://doi.org/10.1126/sciimmunol.aan5357
19. Deng S, Graham ML, Chen X-M. 2023. The complexity of interferon signaling in host defense against protozoan parasite infection. Pathogens 12:319. https://doi.org/10.3390/pathogens12020319
20. Prokunina-Olsson L, Morrison RD, Obajemu A, Mahamar A, Kim S, Attaher O, Florez-Vargas O, Sidibe Y, Onabajo OO, Hutchinson AA, Manning M, Kwan J, Brand N, Dicko A, Fried M, Albert PS, Mbulaiteye SM, Duffy PE. 2021. IFN-λ4 is associated with increased risk and earlier occurrence of several common infections in African children. Genes Immun 22:44–55. https://doi.org/10.1038/s41435-021-00127-7
21. Murillo-León M, Bastidas-Quintero AM, Endres NS, Schnepf D, Delgado-Betancourt E, Ohnemus A, Taylor GA, Schwemmle M, Staeheli P, Steinfeldt T. 2023. IFN-λ is protective against lethal oral *Toxoplasma gondii* infection. bioRxiv:2023.02.24.529861. https://doi.org/10.1101/2023.02.24.529861
22. De M, Bhushan A, Grubbe WS, Roy S, Mendoza JL, Chinnaswamy S. 2022. Distinct molecular phenotypes involving several human diseases are induced by IFN-λ3 and IFN-λ4 in monocyte-derived macrophages. Genes Immun 23:73–84. https://doi.org/10.1038/s41435-022-00164-w
23. Saha S, Roy S, Dutta A, Jana K, Ukil A. 2021. *Leishmania donovani* targets host transcription factor NRF2 to activate antioxidant enzyme HO-1 and transcriptional repressor ATF3 for establishing infection. Infect Immun 89:e0076420. https://doi.org/10.1128/IAI.00764-20
24. Roy DG, Singh L, Chaturvedi HK, Chinnaswamy S. 2023. Gender-dependent multiple cross-phenotype association of interferon lambda genetic variants with peripheral blood profiles in healthy individuals. Mol Genet Genomic Med:e2292. https://doi.org/10.1002/mgg3.2292
25. Titus RG, Marchand M, Boon T, Louis JA. 1985. A limiting dilution assay for quantifying leishmania major in tissues of infected mice. Parasite Immunol 7:545–555. https://doi.org/10.1111/j.1365-3024.1985.tb00098.x
26. Bretagne S, Durand R, Olivi M, Garin JF, Sulahian A, Rivollet D, Vidaud M, Deniau M. 2001. Real-time PCR as a new tool for quantifying leishmania infantum in liver in infected mice. Clin Diagn Lab Immunol 8:828–831. https://doi.org/10.1128/CDLI.8.4.828-831.2001
27. Roy M, Sarkar D, Chatterjee M. 2022. Quantitative monitoring of experimental and human leishmaniasis employing amastigote-specific genes. Parasitology 149:1085–1093. https://doi.org/10.1017/S0031182022000610
28. Mousavi T, Shokohi S, Abdi J, Naserifar R, Ahmadi M, Mirzaei A. 2018. Determination of genetic diversity of Leishmania species using mini-circle kDNA, in Iran-Iraq countries border. Trop Parasitol 8:77–82. https://doi.org/10.4103/tp.TP_3_18
29. Sevilha-Santos L, Dos Santos Júnior ACM, Medeiros-Silva V, Bergmann JO, da Silva EF, Segato LF, Arabi AYM, de Paula NA, Sampaio RNR, Lima BD, Gomes CM. 2019. Accuracy of qPCR for quantifying leishmania kDNA in different skin layers of patients with American tegumentary leishmaniasis. Clin Microbiol Infect 25:242–247. https://doi.org/10.1016/j.cmi.2018.04.025
30. Sacks D, Noben-Trauth N. 2002. The immunology of susceptibility and resistance to leishmania major in mice. Nat Rev Immunol 2:845–858. https://doi.org/10.1038/nri933
31. Streit JA, Donelson JE, Agey MW, Wilson ME. 1996. Developmental changes in the expression of *Leishmania* chagasi gp63 and heat shock

protein in a human macrophage cell line. Infect Immun 64:1810–1818. https://doi.org/10.1128/iai.64.5.1810-1818.1996
32. Burza S, Croft SL, Boelaert M. 2018. Leishmaniasis. Lancet 392:951–970. https://doi.org/10.1016/S0140-6736(18)31204-2
33. Chinnaswamy S. 2014. Genetic variants at the IFNL3 locus and their association with hepatitis C virus infections reveal novel insights into host-virus interactions. J Interferon Cytokine Res 34:479–497. https://doi.org/10.1089/jir.2013.0113
34. Roy S, Guha Roy D, Bhushan A, Bharatiya S, Chinnaswamy S. 2021. Functional genetic variants of the IFN-λ3 (IL28B) gene and transcription factor interactions on its promoter. Cytokine 142:155491. https://doi.org/10.1016/j.cyto.2021.155491
35. Andreakos E, Zanoni I, Galani IE. 2019. Lambda interferons come to light: dual function cytokines mediating antiviral immunity and damage control. Curr Opin Immunol 56:67–75. https://doi.org/10.1016/j.coi.2018.10.007
36. Lu Y-F, Goldstein DB, Urban TJ, Bradrick SS. 2015. Interferon-λ4 is a cell-autonomous type III interferon associated with pre-treatment hepatitis C virus burden. Virology 476:334–340. https://doi.org/10.1016/j.virol.2014.12.020
37. Su Q-J, Wang X, Zhou R-H, Guo L, Liu H, Li J-L, Ho W-Z. 2018. IFN-λ4 inhibits HIV infection of macrophages through signalling of IFN-λR1/IL-10R2 receptor complex. Scand J Immunol 88:e12717. https://doi.org/10.1111/sji.12717
38. Hamming OJ, Terczyńska-Dyla E, Vieyres G, Dijkman R, Jørgensen SE, Akhtar H, Siupka P, Pietschmann T, Thiel V, Hartmann R. 2013. Interferon lambda 4 signals via the IFNLambda receptor to regulate antiviral activity against HCV and coronaviruses. EMBO J 32:3055–3065. https://doi.org/10.1038/emboj.2013.232
39. Obajemu AA, Rao N, Dilley KA, Vargas JM, Sheikh F, Donnelly RP, Shabman RS, Meissner EG, Prokunina-Olsson L, Onabajo OO. 2017. IFN-lambda4 attenuates antiviral responses by enhancing negative regulation of IFN signaling. J Immunol 199:3808–3820. https://doi.org/10.4049/jimmunol.1700807
40. Onabajo OO, Muchmore B, Prokunina-Olsson L. 2019. The IFN-λ4 conundrum: when a good interferon goes bad. J Interferon Cytokine Res 39:636–641. https://doi.org/10.1089/jir.2019.0044
41. Ank N, West H, Bartholdy C, Eriksson K, Thomsen AR, Paludan SR. 2006. Lambda interferon (IFN-lambda), a type III IFN, is induced by viruses and Ifns and displays potent antiviral activity against select virus infections *in vivo*. J Virol 80:4501–4509. https://doi.org/10.1128/JVI.80.9.4501-4509.2006
42. Odendall C, Voak AA, Kagan JC. 2017. Type III IFNs are commonly induced by bacteria-sensing TLRs and reinforce epithelial barriers during infection. J Immunol 199:3270–3279. https://doi.org/10.4049/jimmunol.1700250
43. Cohen TS, Prince AS. 2013. Bacterial pathogens activate a common inflammatory pathway through IFNlambda regulation of PDCD4. PLoS Pathog 9:e1003682. https://doi.org/10.1371/journal.ppat.1003682
44. Hahn WO, Pepper M, Liles WC. 2020. B cell intrinsic expression of IFNλ receptor suppresses the acute humoral immune response to experimental blood-stage malaria. Virulence 11:594–606. https://doi.org/10.1080/21505594.2020.1768329
45. Ferguson SH, Foster DM, Sherry B, Magness ST, Nielsen DM, Gookin JL. 2019. Interferon-λ3 promotes epithelial defense and barrier function against cryptosporidium parvum infection. Cell Mol Gastroenterol Hepatol 8:1–20. https://doi.org/10.1016/j.jcmgh.2019.02.007
46. Gibson AR, Sateriale A, Dumaine JE, Engiles JB, Pardy RD, Gullicksrud JA, O'Dea KM, Doench JG, Beiting DP, Hunter CA, Striepen B. 2022. A genetic screen identifies a protective type III interferon response to cryptosporidium that requires TLR3 dependent recognition. PLoS Pathog 18:e1010003. https://doi.org/10.1371/journal.ppat.1010003
47. Chinnaswamy S, Kowalski ML. 2019. The genetic association of IFN-λs with human inflammatory disorders remains a conundrum. J Interferon Cytokine Res 39:594–598. https://doi.org/10.1089/jir.2019.0009
48. Eslam M, McLeod D, Kelaeng KS, Mangia A, Berg T, Thabet K, Irving WL, Dore GJ, Sheridan D, Grønbæk H, et al. 2017. IFN-λ3, not IFN-λ4, likely mediates IFNL3–IFNL4 haplotype—dependent hepatic inflammation and fibrosis. Nat Genet 49:795–800. https://doi.org/10.1038/ng.3836
49. Kumar R, Bunn PT, Singh SS, Ng SS, Montes de Oca M, De Labastida Rivera F, Chauhan SB, Singh N, Faleiro RJ, Edwards CL, et al. 2020. Type I interferons suppress anti-parasitic immunity and can be targeted to improve treatment of visceral leishmaniasis. Cell Rep 30:2512–2525. https://doi.org/10.1016/j.celrep.2020.01.099
50. Dias BT, Goundry A, Vivarini AC, Costa TFR, Mottram JC, Lopes UG, Lima A. 2022. Toll-like receptor- and protein kinase R-induced type I interferon sustains infection of *Leishmania donovani* in macrophages. Front Immunol 13:801182. https://doi.org/10.3389/fimmu.2022.801182